Vol. 8, no. 4, 2024 eISSN 2587-8999
PEER-REVIEWED SCIENTIFIC AND THEORETICAL JOURNAL

Computational Mathematics and Information Technologies

Computational Mathematics

Mathematical Modelling

Information Technologies

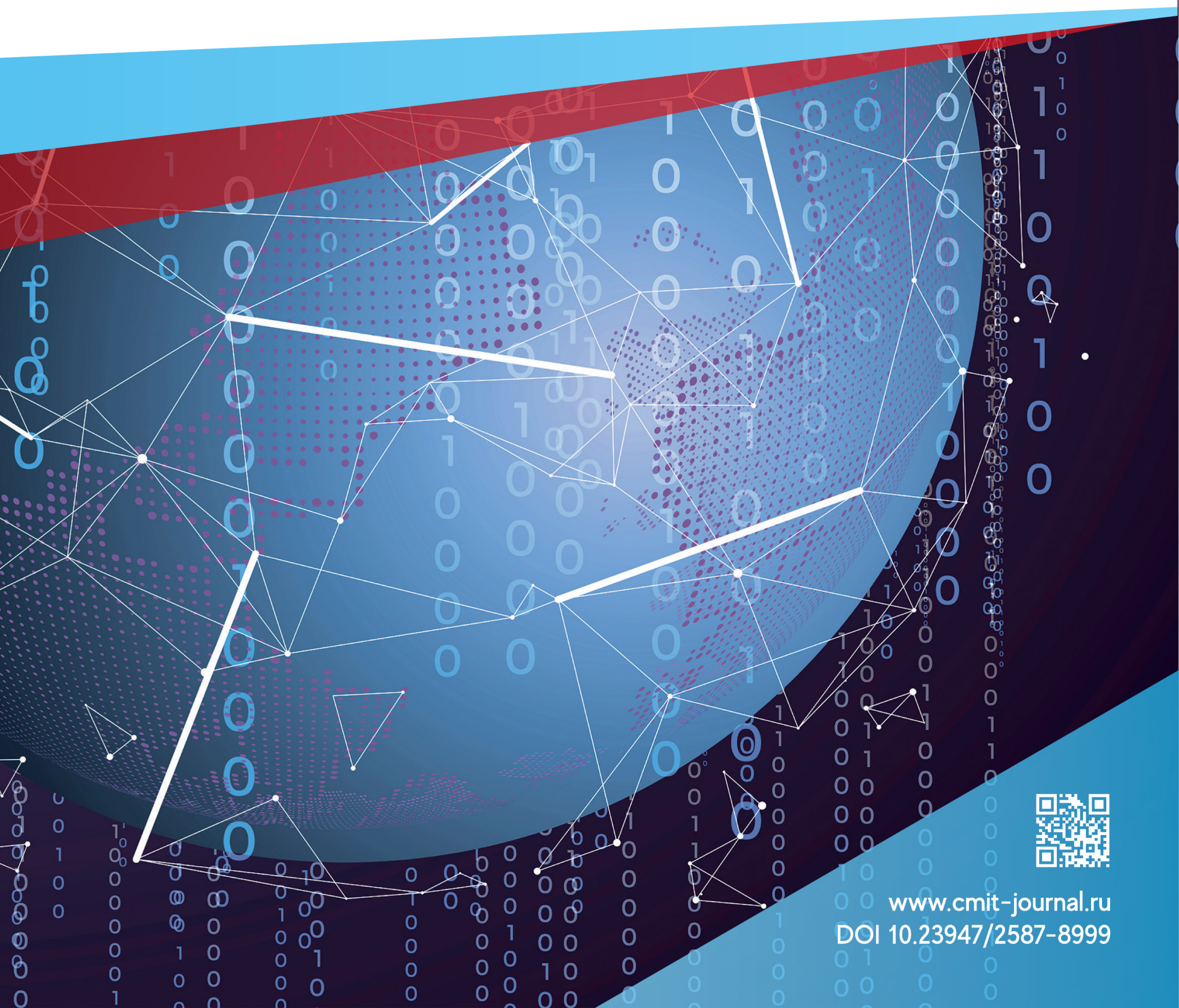

www.cmit-journal.ru
DOI 10.23947/2587-8999

Computational Mathematics and Information Technologies

Peer-reviewed scientific and theoretical journal

eISSN 2587-8999
Published since 2017
Periodicity — 4 issues per year
DOI: 10.23947/2587–8999

Founder and Publisher — Don State Technical University (DSTU), Rostov-on-Don, Russian Federation

The journal “Computational Mathematics and Information Technologies” publishes reviews, original articles and short reports on mathematical modeling, numerical methods and information technologies for solving complex and topical problems of science and modern technology. Research areas include continuum mechanics, fluid dynamics, Earth sciences, chemistry, biology, image processing and pattern recognition, parallel computing theory and its applications, big database and artificial intelligence technologies, etc.

The journal “Computational Mathematics and Information Technologies” accepts scientific and review articles for publication in accordance with the sections:

1. Computational Mathematics
2. Mathematical Modelling
3. Information Technologies

Registration:	Mass media registration certificate ЭЛ № ФС 77–66529 dated July 21, 2016 issued by the Federal Service for Supervision of Communications, Information Technology and Mass Media
Indexing and Archiving:	RISC, Crossref, Cyberleninka
Website:	https://cmit-journal.ru
Address of the Editorial Office:	1, Gagarin sq., Rostov-on-Don, 344003, Russian Federation
E-mail:	CMIT-EJ@yandex.ru
Telephone:	+7 (863) 273–85–14
Date of publication No. 4, 2024:	30.12.2024

Computational Mathematics and Information Technologies

Рецензируемый научно-теоретический журнал

eISSN 2587-8999
Издается с 2017 года
Периодичность — 4 выпуска в год
DOI: 10.23947/2587–8999

Учредитель и издатель — Федеральное государственное бюджетное образовательное учреждение высшего образования «Донской государственный технический университет» (ДГТУ), г. Ростов-на-Дону, Российская Федерация

Журнал «Computational Mathematics and Information Technologies» публикует обзоры, оригинальные статьи и краткие сообщения, посвященные математическому моделированию, численным методам и информационным технологиям для решения сложных и актуальных проблем науки и современной технологии. Область применения исследований — это механика сплошных сред, гидроаэродинамика, науки о Земле, химия, биология, обработка изображений и распознавание образов, теория параллельных вычислений и ее приложения, технологии больших баз данных и искусственного интеллекта и т. д.

Журнал «Computational Mathematics and Information Technologies» принимает к публикации научные и обзорные статьи в соответствии с разделами:

1. Вычислительная математика
2. Математическое моделирование
3. Информационные технологии

Регистрация:	Свидетельство о регистрации средства массовой информации ЭЛ № ФС 77 – 66529 от 21 июля 2016 г., выдано Федеральной службой по надзору в сфере связи, информационных технологий и массовых коммуникаций
Индексация и архивация:	РИНЦ, CrossRef, CyberLeninka
Сайт:	https://cmit-journal.ru
Адрес редакции:	344003, Российская Федерация, г. Ростов-на-Дону, пл. Гагарина, 1
E-mail:	CMIT-EJ@yandex.ru
Телефон:	+7 (863) 273–85–14
Дата выхода № 4, 2024 в свет:	30.12.2024

Contents

Содержание

COMPUTATIONAL MATHEMATICS
ВЫЧИСЛИТЕЛЬНАЯ МАТЕМАТИКА

UDC 519.6

Original Theoretical Research

https://doi.org/10.23947/2587-8999-2024-8-4-7-18

Increasing the Accuracy of Solving Boundary Value Problems with Linear Ordinary Differential Equations Using the Bubnov-Galerkin Method

Natalya K. Volosova[1], Konstantin A. Volosov[2], Aleksandra K. Volosova[2], Mikhail I. Karlov[3], Dmitriy F. Pastukhov[4] ✉, Yuriy F. Pastukhov[4]

[1] MGTU named after N.E. Bauman, Moscow, Russian Federation

[2] Russian University of Transport, Moscow, Russian Federation

[3] Moscow Institute of Physics and Technology (National Research University), Dolgoprudny, Russian Federation

[4] Polotsk State University named after Euphrosyne of Polotsk, Novopolotsk, Republic of Belarus

✉ dmitrij.pastuhov@mail.ru

Abstract

Introduction. This study investigates the possibility of increasing the accuracy of numerically solving boundary value problems using the modified Bubnov-Galerkin method with a linear ordinary differential equation, where the coefficients and the right-hand side are continuous functions. The order of the differential equation n must be less than the number of coordinate functions m.

Materials and Methods. A modified Petrov-Galerkin method was used to numerically solve the boundary value problem. It employs a system of linearly independent power-type basis functions on the interval $[-1,1]$, each normalized by the unit Chebyshev norm. The system of linear algebraic equations includes only the linearly independent boundary conditions of the original problem.

Results. For the first time, an integral quadrature formula with a 22nd order error was developed for a uniform grid. This formula is used to calculate the matrix elements and coefficients in the right-hand side of the system of linear algebraic equations, taking into account the scalar product of two functions based on the new quadrature formula. The study proves a theorem on the existence and uniqueness of a solution for boundary value problems with general non-separated conditions, provided that n linearly independent particular solutions of a homogeneous differential equation of order n are known.

Discussion and Conclusion. The hydrodynamic problem in a viscous strong boundary layer with a third-order equation was precisely solved. The analytical solution was compared with its numerical counterpart, and the uniform norm of their difference did not exceed $5 \cdot 10^{-15}$. The formulas derived using the generalized Bubnov-Galerkin method may be useful for solving boundary value problems with linear ordinary differential equations of the third and higher orders.

Keywords: hydrodynamics, numerical methods, ordinary differential equations, boundary value problems, Galerkin method

For Citation. Volosova N.K., Volosov K.A., Volosova A.K., Karlov M.I., Pastukhov D.F., Pastukhov Yu.F. Increasing the accuracy of solving boundary value problems with a linear differential equation using the Bubnov-Galerkin method. *Computational Mathematics and Information Technologies*. 2024;8(4):7–18. https://doi.org/10.23947/2587-8999-2024-8-4-7-18

Оригинальное теоретическое исследование

Увеличение точности решения краевых задач с линейными обыкновенными дифференциальными уравнениями методом Бубнова-Галеркина

Н.К. Волосова[1], К.А. Волосов[2], А.К. Волосова[2], М.И. Карлов[3], Д.Ф. Пастухов[4]✉, Ю.Ф. Пастухов[4]

[1] Московский государственный технический университет им. Н.Э. Баумана, г. Москва, Российская Федерация

[2] Российский университет транспорта, г. Москва, Российская Федерация

[3] Московский физико-технический институт (национальный исследовательский университет), г. Долгопрудный, Российская Федерация

[4] Полоцкий государственный университет им. Евфросинии Полоцкой, г. Новополоцк, Республика Беларусь

✉ dmitrij.pastuhov@mail.ru

Аннотация

Введение. Исследуется возможность увеличения точности численного решения краевой задачи модифицированным методом Бубнова-Галеркина с линейным обыкновенным дифференциальным уравнением, в котором коэффициенты и правая часть являются непрерывными функциями. Порядок дифференциального уравнения n должен быть меньше числа координатных функций m.

Материалы и методы. Для численного решения краевой задачи использован модифицированный метод Петрова-Галеркина с системой линейно независимых базисных функций степенного вида на отрезке [–1,1] с единичной нормой Чебышева для каждой функции системы. В систему линейных алгебраических уравнений включены только линейно независимые краевые условия исходной задачи.

Результаты исследования. Впервые построена интегральная квадратурная формула на равномерной сетке с двадцать вторым порядком погрешности для вычисления элементов матрицы и коэффициентов правой части системы линейных алгебраических уравнений с учетом скалярного произведения двух функций по новой квадратурной формуле. Доказана теорема существования и единственности решения краевой задачи с неразделенными краевыми условиями общего вида, если известны n линейно независимых частных решений однородного дифференциального уравнения порядка n.

Обсуждение и заключение. Точно решена гидродинамическая задача в вязком сильном пограничном слое с уравнением третьего порядка. Аналитическое решение сравнено с численным решением, равномерная норма разности решений не превышает $5 \cdot 10^{-15}$. Полученные обобщенным методом Бубнова-Галеркина формулы могут быть полезными для решения краевых задач с линейными обыкновенными дифференциальными уравнениями третьего и более высоких порядков.

Ключевые слова: гидродинамика, численные методы, обыкновенные дифференциальные уравнения, краевые задачи, метод Галеркина

Для цитирования. Волосова Н.К., Волосов К.А., Волосова А.К., Карлов М.И., Пастухов Д.Ф., Пастухов Ю.Ф. Увеличение точности решения краевых задач с линейными обыкновенными дифференциальными уравнениями методом Бубнова-Галеркина. *Computational Mathematics and Information Technologies*. 2024;8(4):7–18. https://doi.org/10.23947/2587-8999-2024-8-4-7-18

Introduction. The most well-known methods for solving boundary value problems for ordinary differential equations on an interval are the shooting method [1] and the tridiagonal matrix algorithm [1]. These methods determine the unknown function on a given grid (grid function) using difference equations. In this study, a boundary value problem in the boundary layer of a viscous incompressible fluid, described by a third-order ordinary differential equation [2–3], is considered, and its numerical solution is obtained in a functional form. The hydrodynamic problem in the viscous boundary layer is solved using the modified Bubnov-Galerkin method [4] with a system of linearly independent basis functions. These basis functions have a simple power form, are defined on the interval [−1,1], and are normalized using the unit Chebyshev norm. The unknown solution function is expanded into a series of linearly independent basis functions. In this study, the existence and uniqueness theorem for a boundary value problem on the interval $[a, b]$ with a linear ordinary differential equation of arbitrary order n is generalized to the case of non-separated boundary conditions.

A new integral quadrature formula for a uniform grid, with the number of intervals being a multiple of twenty, is developed for the first time in this work. The quadrature formula achieves a 22nd order error. Compared to the previous work [4], the new quadrature formula, applied to calculate the matrix elements and coefficients in the right-hand side of the system of linear algebraic equations using the scalar product of two functions, reduces the Chebyshev norm of the problem's error by an order of magnitude. For a third-order equation, the system of linear algebraic equations includes $n-1$ linearly independent boundary conditions and $m-n+1$ orthogonality conditions for the residual of the differential equation to the basis functions [4–5] (n is the order of the ODE, and m is the number of basis functions). An exact solution to the problem [1] with selected parameters was obtained, allowing the computation of the Chebyshev norm of the difference between the exact and numerical solutions. Methods for high-accuracy computations in hydrodynamics are presented in works [6–8].

Materials and Methods

Problem Formulation. Let the unknown function u(x) be continuously differentiable n-times on the interval $u(x) \in C^n[a,b]$, be the solution to a boundary value problem governed by an *n*-th order linear ordinary differential equation with variable coefficients $g_i(x) \in C[a,b], i = \overline{0,n}$:

$$\begin{cases} L[u(x)] = f(x),\ x \in (a,b) \\ L[u(x)] \equiv \left(\sum_{i=0}^{n} g_i(x) \dfrac{d^i}{dx^i} \right) u(x), \end{cases} \tag{1}$$

$$\sum_{i=0}^{n-1} \left(\alpha_\mu^i u^{(i)}(a) + \beta_\mu^i u^{(i)}(b) \right) = \gamma_\mu,\ \mu = \overline{1,n}. \tag{2}$$

In the boundary value problem (1)–(2) the functions $g_i(x)(i = \overline{0,n}), f(x) \in C[a,b]$ are given and continuous on the interval [*a*, *b*]. The boundary conditions (2) are specified as linear forms of the function and its derivatives up to the *n*–1-th order at the points $x = a, x = b$. These conditions are of a general type. For the problem (1) to be well-posed, the total number of boundary conditions must equal *n*. The coefficient matrices $\alpha_\mu^i, \beta_\mu^i, i = \overline{0,n-1}, \mu = \overline{1,n}$, and scalars γ_μ, $\mu = \overline{1,n}$ defining the boundary conditions are given. The relationship between these parameters $\alpha_\mu^i, \beta_\mu^i$ determines the existence and uniqueness of the solution to the boundary value problem (1)–(2).

Theorem 1. Let *n* linearly independent particular solutions of the homogeneous equation (1) be known $U_j(x), j = \overline{1,n}$. Then the boundary value problem (1)–(2) has a unique solution if and only if the following condition is satisfied: $\det A_{\mu j} \neq 0, \mu = \overline{1,n}, j = \overline{1,n}$, where $A_{\mu j} = \sum_{i=0}^{n-1} \left(\alpha_\mu^i U_j^{(i)}(a) + \beta_\mu^i U_j^{(i)}(b) \right), \mu, j = \overline{1,n}.$

Proof. The general solution of the linear inhomogeneous equation (1) is given by:

$$u(x) = \sum_{j=1}^{n} U_j(x) D_j + \overline{u(x)},\ j = \overline{1,n},$$

where D_j are arbitrary constants of integration, $\overline{u(x)}$ is a particular solution of the inhomogeneous equation (1), and $L[\overline{u(x)}] = f(x)$; $U_j(x)$ are linearly independent particular solutions of the corresponding homogeneous equation $L[U_j(x)] = 0, j = 1, n$.

Substituting the solution *u*(*x*) into the boundary conditions (2) gives:

$$\begin{gathered} \sum_{i=0}^{n-1} \left(\alpha_\mu^i u^{(i)}(a) + \beta_\mu^i u^{(i)}(b) \right) = \sum_{i=0}^{n-1} \left[\alpha_\mu^i \left(\sum_{j=1}^{n} U_j^{(i)}(a) D_j + \overline{u^{(i)}(a)} \right) + \beta_\mu^i \left(\sum_{j=1}^{n} U_j^{(i)}(b) D_j + \overline{u^{(i)}(b)} \right) \right] = \gamma_\mu \Leftrightarrow \\ \sum_{j=1}^{n} \left(\sum_{i=0}^{n-1} \alpha_\mu^i U_j^{(i)}(a) + \beta_\mu^i U_j^{(i)}(b) \right) D_j = \gamma_\mu - \sum_{i=0}^{n-1} \alpha_\mu^i \overline{u^{(i)}(a)} + \beta_\mu^i \overline{u^{(i)}(b)}, \mu = \overline{1,n}. \end{gathered} \tag{3}$$

An inhomogeneous system of *n* linear algebraic equations (3) with respect to *n* unknowns $D_j, j = \overline{1,n}$ has a unique solution if and only if the matrix *A* is non-singular, that is, $\det A_{\mu j} \neq 0, \mu = \overline{1,n}, j = \overline{1,n}$,

$$A_{\mu j} = \sum_{i=0}^{n-1} \left(\alpha_\mu^i U_j^{(i)}(a) + \beta_\mu^i U_j^{(i)}(b) \right), \mu, j = \overline{1,n}. \tag{4}$$

Theorem 1 is proven. It should be noted that Theorem 1 generalizes Statement 1 from the work [4, p. 25] for the case of separated boundary conditions. In the works on hydrodynamics [2–3], T.Ya. Ershova presents a two-dimensional hydrodynamic problem for a viscous layer, taking into account the continuity equation in incompressible fluid and the fluid dynamics equation, which is reduced, using self-similar variables, to a third-order differential equation in the strong boundary layer:

$$\begin{cases} Lu \equiv \varepsilon u'''(x) + r u''(x) = f(x),\ x \in (0,1), \varepsilon \in (0,1),\ r = const > 0, \\ u(0) = 0,\ u(1) = 0,\ u'(1) = 0. \end{cases} \tag{5}$$

We will solve problem (5) analytically for a particular case of the right-hand side of the equation $f(x) \equiv 1, \varepsilon u'''(x) + r u''(x) \equiv 1,\ z(x) = u''(x),\ \ \varepsilon z'(x) + r z(x) = 1$.

Let us write the general solution of the homogeneous equation $\varepsilon z'(x) + rz(x) = 0 \Leftrightarrow z'(x) = -\frac{r}{\varepsilon} z(x) \Leftrightarrow z(x) = C_0 \exp\left(-\frac{r}{\varepsilon} x\right)$.

By integrating the last solution twice, we obtain $u'(x) = \int z(x)dx = -C_0 \frac{\varepsilon}{r} \exp\left(-\frac{r}{\varepsilon} x\right) + C_1, u(x) = \int u'(x)dx = C_0 \frac{\varepsilon^2}{r^2} \exp\left(-\frac{r}{\varepsilon} x\right) + C_1 x + C_2$.

A particular solution of the equation $\varepsilon u'''(x) + ru''(x) \equiv 1$ is sought in the form:

$$\overline{u(x)} = Cx^2, \overline{u}'''(x) = 0,\ 2rC = 1 \Leftrightarrow C = \frac{1}{2r},\ \overline{u(x)} = \frac{x^2}{2r},$$

$$u_{он}(x) = u_{оо}(x) + \overline{u(x)} = C_0 \frac{\varepsilon^2}{r^2} \exp\left(-\frac{r}{\varepsilon} x\right) + C_1 x + C_2 + \frac{x^2}{2r}, u'_{он}(x) = -C_0 \frac{\varepsilon}{r} \exp\left(-\frac{r}{\varepsilon} x\right) + C_1 + \frac{x}{r}. \tag{6}$$

Function (6) is the general solution of equation (5) with the right-hand side $f(x) \equiv 1$. We apply the boundary conditions of problem (5):

$$u(0) = 0 \Leftrightarrow C_0 \frac{\varepsilon^2}{r^2} + C_2 = 0 \Leftrightarrow C_2 = -C_0 \frac{\varepsilon^2}{r^2}.$$

$$u(1) = 0 \Leftrightarrow C_0 \frac{\varepsilon^2}{r^2} \exp\left(-\frac{r}{\varepsilon}\right) + C_1 + C_2 + \frac{1}{2r} = 0, u'(1) = 0 \Leftrightarrow -C_0 \frac{\varepsilon}{r} \exp\left(-\frac{r}{\varepsilon}\right) + C_1 + \frac{1}{r} = 0.$$

Then

$$C_1 = C_0 \frac{\varepsilon}{r} \exp\left(-\frac{r}{\varepsilon}\right) - \frac{1}{r},\ \ C_0 \frac{\varepsilon^2}{r^2} \exp\left(-\frac{r}{\varepsilon}\right) + C_1 + C_2 + \frac{1}{2r} = 0 \Leftrightarrow$$

$$C_0 \frac{\varepsilon^2}{r^2} \exp\left(-\frac{r}{\varepsilon}\right) + C_0 \frac{\varepsilon}{r} \exp\left(-\frac{r}{\varepsilon}\right) - \frac{1}{r} - C_0 \frac{\varepsilon^2}{r^2} + \frac{1}{2r} = 0 \Leftrightarrow C_0 = \frac{r}{2\left(\left(\varepsilon^2 + \varepsilon r\right)\exp\left(-\frac{r}{\varepsilon}\right) - \varepsilon^2\right)},$$

$$C_2 = -C_0 \frac{\varepsilon^2}{r^2} = \frac{\varepsilon^2}{2r\left(\varepsilon^2 - \left(\varepsilon^2 + \varepsilon r\right)\exp\left(-\frac{r}{\varepsilon}\right)\right)}, C_1 = \frac{\varepsilon \exp\left(-\frac{r}{\varepsilon}\right)}{2\left(\left(\varepsilon^2 + \varepsilon r\right)\exp\left(-\frac{r}{\varepsilon}\right) - \varepsilon^2\right)} - \frac{1}{r}.$$

As a result, we obtain:

$$u(x) = \frac{\varepsilon^2 \exp\left(-\frac{r}{\varepsilon} x\right)}{2r\left(\left(\varepsilon^2 + \varepsilon r\right)\exp\left(-\frac{r}{\varepsilon}\right) - \varepsilon^2\right)} + \left(\frac{\varepsilon \exp\left(-\frac{r}{\varepsilon}\right)}{2\left(\left(\varepsilon^2 + \varepsilon r\right)\exp\left(-\frac{r}{\varepsilon}\right) - \varepsilon^2\right)} - \frac{1}{r}\right) x + \frac{\varepsilon^2}{2r\left(\varepsilon^2 - \left(\varepsilon^2 + \varepsilon r\right)\exp\left(-\frac{r}{\varepsilon}\right)\right)} + \frac{x^2}{2r}. \tag{7}$$

For testing the program using the Bubnov-Galerkin algorithm [2–4], we choose the parameters $r = 1$, $\varepsilon = 1/2$, and from formula (7) we obtain the function (8).

$$u(x) = \frac{\exp(2 - 2x)}{2(3 - e^2)} + \frac{(e^2 - 2)x}{(3 - e^2)} - \frac{e^2}{2(3 - e^2)} + \frac{x^2}{2}. \tag{8}$$

As in the work [4], we choose a system of basis functions $\phi_i(x), i = \overline{0,m},\ m > n$, that is linearly independent.

$$\{\phi_i(x)\}_{i=0}^m = \left\{\left(\frac{2x - a - b}{b - a}\right)^i, x \in [a,b], i = \overline{0,m}\right\}, \|\phi_i(x)\|_C = \max_{x\in[a,b]} |\phi_i(x)| = 1 \forall i = \overline{0,m}. \tag{9}$$

A linear transformation $z = \frac{2x - a - b}{b - a}, z \in [-1,1]$ bijectively maps the interval [a, b] to the interval [–1,1]. The basis functions $\phi_i(x)$ with even indices are even on the interval [–1,1], while those with odd indices are odd. Let the midpoint of the interval [a, b] be denoted by $c = (a + b)/2$. We expand the solution of the general problem (1) in terms of the system of basis functions (9):

$$u(x) = u(c) + \sum_{j=1}^m \phi_j(x) D_j = u(c) + \sum_{j=1}^m \left(\frac{2(x - c)}{b - a}\right)^j D_j. \tag{10}$$

From formula (10), the identity follows $u(c) = u(c)$, and formula (10) itself is the expansion of the unknown function in a power series centered at $x = c = (a + b)/2$.

Note. The Bubnov-Galerkin method is orthogonal. However, it does not require the system of basis functions to be orthogonal polynomials, such as Legendre polynomials on the interval [–1,1] with a weight function $\rho(z) \equiv 1$, $z \in [-1,1]$. The system of functions (9) must be linearly independent. It should be noted that the orthogonality of the system of functions (9) in the residual of the differential equation in problem (1) is expressed with the weight function $\rho(z) \equiv 1$, $z \in [-1,1]$. Moreover, finding derivatives of any order from functions (9) is significantly easier than from Legendre polynomials.

Substitute (10) into equation (1) and write the residual of equation (1):

$$R(u((x)) = L[u(x)] - f(x) = L\left(u(c) + \sum_{j=1}^{m}\phi_j(x)D_j\right) - f(x) = L\left(u(c)\right) + \sum_{j=1}^{m} L\phi_j(x)D_j - f(x).$$

According to the Bubnov-Galerkin method, we write the orthogonality conditions of the residual with respect to the maximum number of coordinate functions $\left\{1, z, z^2, ..., z^{m-3}\right\}$, for solving problem (5) with the third-order equation, which contributes the most to the residual of equation (5) (for m–n+1 functions in the general problem (1)):

$$\left\langle R\left(u(x)\right), \phi_i(x)\right\rangle = 0, i = \overline{0, m-3} \Leftrightarrow \sum_{j=1}^{n}\left\langle L\phi_j(x), \phi_i(x)\right\rangle D_j = \left\langle f(x) - L\left(u(c)\right), \phi_i(x)\right\rangle, i = \overline{0, m-3}, \tag{11}$$

In formula (11), the symbol $\langle q, g\rangle$ denotes the scalar product of functions:

$$\left\langle q, g\right\rangle = \int_a^b q(x)g(x)dx, \ L\left(u(c)\right) = g_0(x)u(c) = g_0(x)u_c. \tag{12}$$

To ensure the closure of the system (11), two additional equations are required. As shown in work [9], the boundary value problem requires that the solution belongs to the class of admissible functions, meaning that all linearly independent boundary conditions should be used. At the endpoints of the interval $x = a$, $x = b$, using formula (10), we obtain:

$$u(a) \equiv u_a = u(c) + \sum_{j=1}^{m}\left(\frac{(2a-a-b}{b-a}\right)^j D_j = u_c + \sum_{j=1}^{m}\left(-1\right)^j D_j, u(b) \equiv u_b = u(c) + \sum_{j=1}^{m}\left(\frac{(2b-a-b}{b-a}\right)^j D_j = u_c + \sum_{j=1}^{m} D_j.$$

By summing the last two equations and expressing $u(c) = u_c$, we get

$$u_c = \left(\frac{u_a + u_b}{2}\right) - D_2 - D_4 - ... - \begin{cases} D_m, m = 2l \\ D_{m-1}, m = 2l+1. \end{cases} \tag{13}$$

Similarly, expressing $\frac{u_b - u_a}{2}$, we obtain the formula:

$$\frac{u_b - u_a}{2} = D_1 + D_3 + ... + \begin{cases} D_{m-1}, m = 2l \\ D_m, m = 2l+1. \end{cases} \tag{14}$$

We compute the first derivative $u(x)$ from formula (10) and set it to zero at the point $x = b$ according to the boundary condition of problem (5):

$$u'(x) = \sum_{j=1}^{m}\phi'_j(x)D_j = \sum_{j=1}^{m}\frac{2j}{(b-a)}\left(\frac{(2x-a-b}{b-a}\right)_{x=b}^{j-1} D_j = 0 \Leftrightarrow D_1 + 2D_2 + 3D_3 + ... + mD_m = 0. \tag{15}$$

Substitute the value of $u(c)$ from formula (13) into the right-hand side of equation (11), then move all terms containing D_j to the left-hand side of equation (11). Taking into account formulas (14) and (15), we obtain a system of linear algebraic equations (16) for the unknown coefficients D_j

$$\sum_{j=1}^{m} a_{i,j}D_j = \overline{f_i}, \ i = \overline{0, m-1}, \tag{16}$$

where the elements of the matrix $a_{i,j}, i = \overline{0, m-1}, j = \overline{1, m}$ and the coefficients of the right-hand side $\overline{f_i}$ of system (16) are given as:

$$a_{i,j} = \begin{cases} \left\langle L\phi_j, \phi_i\right\rangle, \text{ if } j \equiv 1\left(\bmod 2\right), i = \overline{0, m-3} \\ \left\langle L\left(\phi_j - 1\right), \phi_i\right\rangle, \text{ if } j \equiv 0\left(\bmod 2\right), i = \overline{0, m-3} \\ 1, \text{ if } i = m-2, j \equiv 1\left(\bmod 2\right) \\ 0, \text{ if } i = m-2, j \equiv 0\left(\bmod 2\right) \\ j, \text{ if } i = m-1 \end{cases},$$

$$\overline{f_i} = \begin{cases} \left\langle f(x) - L\left(\frac{u_a+u_b}{2}\right), \phi_i(x) \right\rangle, \text{ if } i = \overline{0, m-3}, L\left(\frac{u_a+u_b}{2}\right) = \left(\frac{u_a+u_b}{2}\right) g_0(x) \\ \frac{u_b-u_a}{2}, \text{ if } i = m-2 \\ 0, \text{ if } i = m-1 \end{cases},$$

The action of a third-order linear differential operator in problem (5) on a basis function with index j can be represented by the system of formulas (17):

$$L\phi_j = \begin{cases} g_0(x), \text{ if } j=0, \\ \frac{2g_1(x)}{(b-a)} + g_0(x)\left(\frac{2x-a-b}{b-a}\right), \text{ if } j=1, \\ 8g_2(x)\frac{1}{(b-a)^2} + +4g_1(x)\frac{(2x-a-b)}{(b-a)^2} + g_0(x)\left(\frac{2x-a-b}{b-a}\right)^2, \text{ if } j=2, \\ 8j(j-1)(j-2)g_2(x)\frac{(2x-a-b)^{j-3}}{(b-a)^j} + 4j(j-1)g_2(x)\frac{(2x-a-b)^{j-2}}{(b-a)^j} + \\ +2jg_1(x)\frac{(2x-a-b)^{j-1}}{(b-a)^j} + g_0(x)\frac{(2x-a-b)^j}{(b-a)^j}, \text{ if } j \ge 3. \end{cases}$$

The numerical solution of problem (5) is obtained by substituting (13) into formula (10), resulting in the expression (18):

$$u(x) = \left(\frac{u_a+u_b}{2}\right) + \sum_{j=1}^{m}\left[\left(\frac{(2x-a-b}{b-a}\right)^j + \left(\frac{-1+(-1)^{j+1}}{2}\right)\right] D_j. \tag{18}$$

In solution (18), the unknown vector D is determined from the system of linear algebraic equations (16) $D = A^{-1}\overline{f}.$. The estimate of the uniform norm of the solution $u(x)$ yields the following result:

$$|u(x)| \le \frac{|u_a|+|u_b|}{2} + 2\sum_{j=1}^{m}|D_j| \le \frac{|u_a|+|u_b|}{2} + 2m\max_{j=1,m} D_j = \frac{|u_a|+|u_b|}{2} + 2m\|D\|_C \le \frac{|u_a|+|u_b|}{2} + 2m\|A^{-1}\|_C \|\overline{f}\|_C \Rightarrow$$

$$\|u\|_C \le \frac{|u_a|+|u_b|}{2} + 2m\|A^{-1}\|_C \|\overline{f}\|_C.$$

where the norm of the inverse matrix A^{-1} is determined by the formula $\|A^{-1}\|_C = \max_{i=1,m}\sum_{j=1}^{m}|a_{i,j}^{-1}|$.

In work [4], to compute all matrix elements $a_{i,j}$, and the coefficients of the right-hand side $\overline{f_i}$ of the system of linear algebraic equations (16) through the scalar product of two functions (12), a composite quadrature integral formula (19) with a uniform step and 12th-order error $O(h^{12})$ was applied. This formula was used by the program for the numerical solution of test example 3:

$$\langle y_1, y_2 \rangle = \int_a^b y_1(x)y_2(x)dx = 5h\sum_{i=0}^{n_1} y_1(x_i)\, y_2(x_i) C_i + O(h^{12}), n_1 = 10p, h = \frac{b-a}{n_1}, p \in N, \tag{19}$$

where the weight coefficients of the integral quadrature formula (19) are determined by the remainder of the division of the node index i on the uniform grid by 10.

$$C_i = \begin{cases} \frac{16067}{299376}, i = 0 \vee i = n_1, \\ \frac{16067}{149688}, (i \equiv 0 \bmod 10) \wedge (0 < i < n_1), \\ \frac{26575}{74844}, (i \equiv 1 \bmod 10) \vee (i \equiv 9 \bmod 10), \\ \frac{-16175}{99792}, (i \equiv 2 \bmod 10) \vee (i \equiv 8 \bmod 10), \\ \frac{5675}{6237}, (i \equiv 3 \bmod 10) \vee (i \equiv 7 \bmod 10), \\ \frac{-4825}{5544}, (i \equiv 4 \bmod 10) \vee (i \equiv 6 \bmod 10), \\ \frac{17807}{12474}, i \equiv 5 \bmod 10. \end{cases} \tag{20}$$

Applying the scalar product formula for two functions using formula (19) with weight coefficients (20) and the Petrov-Galerkin algorithm (16)–(18) with $m = 16$ basis functions and $n_1 = 20$ integration intervals, the program computes the uniform norm of the residual in problem (5). The exact solution is calculated using formula (8) on a uniform grid:

$$u_i^{exact}, x_i = a + h \cdot i, i = \overline{0, n_1}, h = \frac{b-a}{n_1},$$

$$\left\| u^{num} - u^{exact} \right\|_C = \max_{i=0,n_1} \left| u_i^{num} - u_i^{exact} \right| \approx 2.016997679987753\text{E–}012.$$

In this study, a novel quadrature integral formula with a uniform step and a 22nd-order error $O(h^{22})$ is proposed for the first time. This formula enhances the accuracy of the scalar product computation and the evaluation of matrix elements and the coefficients of the right-hand side of the system of linear algebraic equations (16), thereby reducing the norm of the residual error in problem (5).

For the quadrature integral formula on a uniform grid [a, b] [1, p. 87], with an error of $O(h^{22})$ and considering symmetry, the quadrature formula is written relative to the midpoint of the interval [a, b]:

$$c = (a+b)/2 \Leftrightarrow z = 0, \quad x = \frac{(a+b)}{2} + \frac{(b-a)}{2} z, z \in [-1,1], x \in [a,b], dx = \frac{(b-a)}{2} dz$$

we obtain:

$$\int_a^b f(x)dx = \frac{(b-a)}{2} \int_{-1}^{1} f(z)dz, \int_{-1}^{1} f(z)dz = C_0 f(0) + \sum_{i=1}^{i=10} C_i \left(f(-z_i) + f(z_i) \right), z_i = i/10. \tag{21}$$

By substituting even-degree power functions into formula (21), we simplify the computations as follows (odd-degree functions result in the trivial identity 0=0) $f(z) = \{0, z^2, z^4, z^6, z^8, z^{10}, z^{12}, z^{14}, z^{16}, z^{18}, z^{20}\}$, we obtain a system of 11 linear inhomogeneous algebraic equations for the variables $C_i, i = \overline{0,10}$:

$$I_{2k} = \int_{-1}^{1} z^{2k} dz = \frac{2}{2k+1} = \begin{cases} C_0 + 2\sum_{i=1}^{10} C_i, k = 0 \\ 2\sum_{i=1}^{10} z_i^{2k} C_i, k = 1,2,3,4,5,6,7,8,9,10; z_i = i/10, i = \overline{1,10}. \end{cases} \tag{22}$$

Results. The system of equations (22) was solved symbolically without rounding using a symbolic computation environment. The coefficients C_i are provided in formula (24), and Table 1 illustrates the comparison between computed and exact values. The table presents the numerical values of $I^{num}{}_k$ (the right-hand side of formula (22)) and the exact values of the integral $I^{exact}{}_k = \frac{1+(-1)^k}{k+1}$ (the left-hand side of formula (22)) for power functions $f(z) = \{1, z, z^2, \ldots z^{21}, z^{22}\}$ on the interval [–1, 1] taking into account the coefficients.

Table 1

Comparison of Numerical and Exact Values

k	$I^{exact}{}_k = \frac{1+(-1)^k}{k+1}$	$I^{num}{}_k$
0	2.00000000000000	2.00000000000003
1	0.000000000000000E+000	1.379105163401562E–015
2	0.666666666666667	0.666666666666679
3	0.000000000000000E+000	2.586472702681419E–015
4	0.400000000000000	0.399999999999999
5	0.000000000000000E+000	–3.694961003830599E–016
6	0.285714285714286	0.285714285714285
7	0.000000000000000E+000	–4.388850394221322E–016
8	0.222222222222222	0.222222222222222
9	0.000000000000000E+000	–1.752070710736575E–016
10	0.181818181818182	0.181818181818181
11	0.000000000000000E+000	–1.613292832658431E–016
12	0.153846153846154	0.153846153846153

End of table 1

k	$I^{exact}{}_k = \dfrac{1+(-1)^k}{k+1}$	$I^{num}{}_k$
13	0.000000000000000E+000	–8.500145032286355E–017
14	0.133333333333333	0.133333333333333
15	0.000000000000000E+000	2.602085213965211E–017
16	0.117647058823529	0.117647058823529
17	0.000000000000000E+000	1.092875789865388E–016
18	0.105263157894737	0.105263157894737
19	0.000000000000000E+000	1.578598363138894E–016
20	9.523809523809523E–002	9.523809523809518E–002
21	0.000000000000000E+000	1.717376241217039E–016
22	8.695652173913043E–002	8.695652174444995E–002

The conditions of the system (22) and Table 1 demonstrate that the quadrature formulas (22) and (23) achieve twenty-second order accuracy.

If

$$b-a=nh, n=20s, s\in N, \left(\frac{b-a}{2}\right)=10sh, x_i=a+i\cdot h,\ i=\overline{0,n},$$

then

$$\int_a^b f(x)dx=10h\sum_{i=0}^{n=20s} C_i f\left(x_i\right)+O\left(h^{22}\right), x_i=a+i\cdot h,\ i=\overline{0,n},$$

The scalar product of two functions, as defined by formulas (19) and (20), is expressed as follows:

$$\left\langle y_1,y_2\right\rangle=\int_a^b y_1(x)y_2(x)dx=10h\sum_{i=0}^{n_1} y_1\left(x_i\right)y_2\left(x_i\right)C_i+O\left(h^{22}\right), n_1=20s, h=\frac{b-a}{n_1}, s\in N, \tag{23}$$

where C_i are the weight coefficients in the composite quadrature integral formula (23), which are obtained by solving the system of linear algebraic equations (22):

$$C_i=\begin{cases}\dfrac{1145302367137}{48426042384720},\ \text{if } i=0 \text{ or } i=n_1,\\ \dfrac{1145302367137}{24213021192360},\ \text{if } \left(i\equiv 0 \bmod 20\right) \text{ and } \left(0<i<n_1\right),\\ \dfrac{335582304250}{1470076286679},\ \text{if} \left(i\equiv 1 \bmod 20\right) \text{ or } \left(i\equiv 19 \bmod 20\right),\\ \dfrac{-19467909708875}{41162136027012},\ \text{if } \left(i\equiv 2 \bmod 20\right) \text{ or } \left(i\equiv 18 \bmod 20\right),\\ \dfrac{8274871497250}{3430178002251},\ \text{if } \left(i\equiv 3 \bmod 20\right) \text{ or } \left(i\equiv 17 \bmod 20\right),\\ \dfrac{-413929922392625}{54882848036016},\ \text{if } \left(i\equiv 4 \bmod 20\right) \text{ or } \left(i\equiv 16 \bmod 20\right),\\ \dfrac{50652939811064}{2450127144465},\ \text{if } \left(i\equiv 5 \bmod 20\right) \text{ or } \left(i\equiv 15 \bmod 20\right),\\ -\dfrac{155790561130375}{3430178002251},\ \text{if } \left(i\equiv 6 \bmod 20\right) \text{ or } \left(i\equiv 14 \bmod 20\right)\\ \dfrac{286955364893000}{3430178002251},\ \text{if } \left(i\equiv 7 \bmod 20\right) \text{ or } \left(i\equiv 13 \bmod 20\right)\\ -\dfrac{502376261017625}{3920203431144},\ \text{if } \left(i\equiv 8 \bmod 20\right) \text{ or } \left(i\equiv 12 \bmod 20\right)\\ \dfrac{1704056522480500}{10290534006753},\ \text{if } \left(i\equiv 9 \bmod 20\right) \text{ or } \left(i\equiv 11 \bmod 20\right)\\ -\dfrac{1684005984173647}{9355030915230},\ \text{if } i\equiv 10 \bmod 20.\end{cases} \tag{24}$$

We will find the characteristic equation and the particular solutions of the homogeneous equation (5) with the chosen parameters:

$$\varepsilon=\frac{1}{2}, r=1, \varepsilon u'''(x)+ru''(x)=\frac{1}{2}u'''(x)+u''(x)=0 \Rightarrow \lambda^3+2\lambda^2=0 \Leftrightarrow \lambda_1=\lambda_2=0, \lambda_3=-2,$$

These correspond to three linearly independent solutions:

$$\left\{U_1(x)=1, U_2(x)=x, U_3(x)=\exp(-2x)\right\}, \left\{U_1'(x)=0, U_2'(x)=1, U_3'(x)=-2\exp(-2x)\right\},$$

$$\left\{U_1''(x)=0, U_2''(x)=0, U_3''(x)=4\exp(-2x)\right\}.$$

Next, we verify the existence and uniqueness of the solution to the boundary value problem (5) with parameters $\varepsilon=\frac{1}{2}, r=1$.

Finally, we compute the elements of the matrix, as defined in formula (4), for solving the system of equations:

$$A_{\mu j}=\sum_{i=0}^{n-1}\left(\alpha_\mu^i U_j^{(i)}(a)+\beta_\mu^i U_j^{(i)}(b)\right), \mu, j=\overline{1,n},\ u(0)=0,\ u(1)=0,\ u'(1)=0 \Leftrightarrow$$

$$\alpha_1^0=1; \alpha_1^1=0; \alpha_1^2=0; \beta_1^0=0; \beta_1^1=0; \beta_1^2=0,$$

$$\alpha_2^0=0; \alpha_2^1=0; \alpha_2^2=0; \beta_2^0=1; \beta_2^1=0; \beta_2^2=0,$$

$$\alpha_3^0=0; \alpha_3^1=0; \alpha_3^2=0; \beta_3^0=0; \beta_3^1=1; \beta_3^2=0,$$

$$A_{11}=\alpha_1^0U_1^{(0)}(0)+\beta_1^0U_1^{(0)}(1)+\alpha_1^1U_1^{(1)}(0)+\beta_1^1U_1^{(1)}(1)+\alpha_1^2U_1^{(2)}(0)+\beta_1^2U_1^{(2)}(1)=1\cdot1+0\cdot1+0\cdot0+0\cdot0+0\cdot0+0\cdot0=1,$$

$$A_{21}=\alpha_2^0U_1^{(0)}(0)+\beta_2^0U_1^{(0)}(1)+\alpha_2^1U_1^{(1)}(0)+\beta_2^1U_1^{(1)}(1)+\alpha_2^2U_1^{(2)}(0)+\beta_2^2U_1^{(2)}(1)=0\cdot1+1\cdot1+0\cdot0+0\cdot0+0\cdot0+0\cdot0=1,$$

$$A_{31}=\alpha_3^0U_1^{(0)}(0)+\beta_3^0U_1^{(0)}(1)+\alpha_3^1U_1^{(1)}(0)+\beta_3^1U_1^{(1)}(1)+\alpha_3^2U_1^{(2)}(0)+\beta_3^2U_1^{(2)}(1)=0\cdot1+0\cdot1+0\cdot0+1\cdot0+0\cdot0+0\cdot0=0,$$

$$A_{12}=\alpha_1^0U_2^{(0)}(0)+\beta_1^0U_2^{(0)}(1)+\alpha_1^1U_2^{(1)}(0)+\beta_1^1U_2^{(1)}(1)+\alpha_1^2U_2^{(2)}(0)+\beta_1^2U_2^{(2)}(1)=1\cdot0+0\cdot1+0\cdot1+0\cdot1+0\cdot0+0\cdot0=0,$$

$$A_{22}=\alpha_2^0U_2^{(0)}(0)+\beta_2^0U_2^{(0)}(1)+\alpha_2^1U_2^{(1)}(0)+\beta_2^1U_2^{(1)}(1)+\alpha_2^2U_2^{(2)}(0)+\beta_2^2U_2^{(2)}(1)=0\cdot0+1\cdot1+0\cdot1+0\cdot1+0\cdot0+0\cdot0=1,$$

$$A_{32}=\alpha_3^0U_2^{(0)}(0)+\beta_3^0U_2^{(0)}(1)+\alpha_3^1U_2^{(1)}(0)+\beta_3^1U_2^{(1)}(1)+\alpha_3^2U_2^{(2)}(0)+\beta_3^2U_2^{(2)}(1)=0\cdot0+0\cdot1+0\cdot1+1\cdot1+0\cdot0+0\cdot0=1,$$

$$A_{13}=\alpha_1^0U_3^{(0)}(0)+\beta_1^0U_3^{(0)}(1)+\alpha_1^1U_3^{(1)}(0)+\beta_1^1U_3^{(1)}(1)+\alpha_1^2U_3^{(2)}(0)+\beta_1^2U_3^{(2)}(1)=1\cdot1+0\cdot e^{-2}+0\cdot(-2)+$$
$$+0\cdot\left(-2e^{-2}\right)+0\cdot4+0\cdot4e^{-2}=1,$$

$$A_{23}=\alpha_2^0U_3^{(0)}(0)+\beta_2^0U_3^{(0)}(1)+\alpha_2^1U_3^{(1)}(0)+\beta_2^1U_3^{(1)}(1)+\alpha_2^2U_3^{(2)}(0)+\beta_2^2U_3^{(2)}(1)=0\cdot1+1\cdot e^{-2}+0\cdot(-2)+$$
$$+0\cdot\left(-2e^{-2}\right)+0\cdot4+0\cdot4e^{-2}=e^{-2},$$

$$A_{33}=\alpha_3^0U_3^{(0)}(0)+\beta_3^0U_3^{(0)}(1)+\alpha_3^1U_3^{(1)}(0)+\beta_3^1U_3^{(1)}(1)+\alpha_3^2U_3^{(2)}(0)+\beta_3^2U_3^{(2)}(1)=0\cdot1+0\cdot e^{-2}+0\cdot(-2)+$$
$$+1\cdot(-2e^{-2})+0\cdot4+0\cdot4e^{-2}=-2e^{-2}.$$

Since $\begin{vmatrix}1 & 0 & 1\\ 1 & 1 & e^{-2}\\ 0 & 1 & -2e^{-2}\end{vmatrix}=\begin{vmatrix}1 & e^{-2}\\ 1 & -2e^{-2}\end{vmatrix}+\begin{vmatrix}1 & 1\\ 0 & 1\end{vmatrix}=-3e^{-2}+1\neq0,$ according to Theorem 1, the boundary value problem (5) with parameters $\varepsilon=\frac{1}{2}, r=1$ has a unique solution. The exact solution with the right-hand side $f(x)\equiv1, \varepsilon=\frac{1}{2}, r=1$ is given by function (8). No other solutions exist.

The inverse matrix A^{-1} in the system of linear algebraic equations (SLAE) (16) is computed using the msimsl linear algebra library to find the coefficient vector D_j, $j = 1, m$. The program, using formulas (16), (17), (18), (23), and (24), provides the numerical solution to problem (5)

$$x_i=a+h\cdot i, i=\overline{0,n_1}, h=\frac{b-a}{n_1}, n_1=20, a=0, b=1.$$

with parameters $\varepsilon=\frac{1}{2}, r=1, f(x)\equiv1, g_3(x)=\varepsilon=\frac{1}{2}, g_2(x)=r=1, g_1(x)=0, g_0(x)=0,$ as presented in Table 2. The number of basis functions is $m = 18$.

Table 2

Numerical u_i^{num} and Exact u_i^{exact} Solutions to Problem (5)

x_i	u_i^{num}	u_i^{exact}	$u_i^{num} - u_i^{exact}$
0.000000E+000	0.0000000000E+000	0.00000000000E+000	0.00000000E+000
5.0000000E-002	1.99620012886537E–002	1.99620012886524E–002	1.231653667E–015
0.1000000000	3.48011017443269E–002	3.48011017443259E–002	1.006139616E–015
0.1500000000	4.52427162923431E–002	4.52427162923431E–002	6.938893903E–018
0.2000000000	5.19432275007362E–002	5.19432275007366E–002	–3.816391647E–016
0.2500000000	5.54965548776091E–002	5.54965548776098E–002	–6.800116025E–016
0.3000000000	5.64400990171948E–002	5.64400990171955E–002	–7.563394355E–016
0.3500000000	5.52601200856299E–002	5.52601200856307E–002	–8.118505867E–016
0.4000000000	5.23966044761353E–002	5.23966044761364E–002	–1.033895191E–015
0.4500000000	4.82476683407243E–002	4.82476683407254E–002	–1.075528555E–015
0.5000000000	4.31735420704626E–002	4.31735420704638E–002	–1.221245327E–015
0.5500000000	3.75001756023005E–002	3.75001756023019E–002	–1.415534356E–015
0.6000000000	3.15225006355969E–002	3.15225006355983E–002	–1.450228825E–015
0.6500000000	2.55073824076967E–002	2.55073824076980E–002	–1.356553758E–015
0.7000000000	1.96962905709227E–002	1.96962905709242E–002	–1.467576060E–015
0.7500000000	1.43077159020167E–002	1.43077159020178E–002	–1.103284130E–015
0.8000000000	9.53935703127063E–003	9.53935703127128E–003	–6.574601973E–016
0.8500000000	5.57009907686709E–003	5.57009907686645E–003	6.435824095E–016
0.9000000000	2.56180398726754E–003	2.56180398726446E–003	3.080001531E–015
0.9500000000	6.609305099950E–004	6.609305099896E–004	5.435105490E–015
1.0000000000	0.0000000000E+000	–1.110223024625157E–016	1.110223024E–016

In the first column of Table 1, the values of the nodes x_i on the uniform grid are given. In the second column, the numerical solution u_i^{num} is recorded, and in the third column, the exact solution u_i^{exact} at the nodes is presented. The last column contains the difference between the numerical and exact solutions $u_i^{num} - u_i^{exact}$.

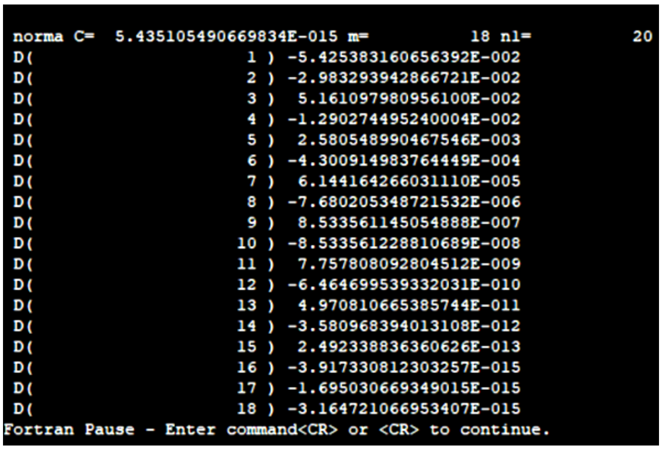

```
norma C=  5.435105490669834E-015 m=          18 n1=          20
D(                    1 ) -5.425383160656392E-002
D(                    2 ) -2.983293942866721E-002
D(                    3 )  5.161097980956100E-002
D(                    4 ) -1.290274495240004E-002
D(                    5 )  2.580548990467546E-003
D(                    6 ) -4.300914983764449E-004
D(                    7 )  6.144164266031110E-005
D(                    8 ) -7.680205348721532E-006
D(                    9 )  8.533561145054888E-007
D(                   10 ) -8.533561228810689E-008
D(                   11 )  7.757808092804512E-009
D(                   12 ) -6.464699539332031E-010
D(                   13 )  4.970810665385744E-011
D(                   14 ) -3.580968394013108E-012
D(                   15 )  2.492338836360626E-013
D(                   16 ) -3.917330812303257E-015
D(                   17 ) -1.695030669349015E-015
D(                   18 ) -3.164721066953407E-015
Fortran Pause - Enter command<CR> or <CR> to continue.
```

Fig. 1. Program Results

Taking into account formulas (23)–(24), the program gives an error norm $\left\| u^{num} - u^{exact} \right\|_C = \max\limits_{i=0,n_1} \left| u_i^{num} - u_i^{exact} \right| \approx 5.435105E–015$ with a result several times smaller than when using the scalar product formulas (19)–(20). Fig. 1 shows that the number of basis functions is optimal when the coefficients decrease in absolute value as their index increases. The advantage of the scalar product formulas (23)–(24) over formulas (19)–(20) also lies in the weak dependence of the error norm on the number of basis functions over a wide range of their values.

Discussion and Conclusion. The theorem of existence and uniqueness of the solution to the boundary value problem with a linear ordinary differential equation of order n has been generalized to the case of non-separated boundary conditions, provided that n linearly independent particular solutions of the corresponding homogeneous equation are

known. The boundary value problem with a third-order differential equation in the boundary layer for an incompressible fluid, with parameters $\varepsilon = 0{,}5$, $r = 1$ and constant right-hand side $f(x) = 1$ has been solved analytically. A Bubnov-Galerkin method with a system of linearly independent basis functions on the interval [–1,1] has been proposed for the numerical solution of the boundary hydrodynamic problem with a strong boundary layer. The basis functions are bounded by the Chebyshev unit norm. A new quadrature integral formula with a uniform step has been introduced for calculating the matrix elements and right-hand side coefficients in the Bubnov-Galerkin method, which results in a second-order error bound. The Chebyshev vector norm for the difference between the exact solution and the numerical solution on a uniform grid, using the scalar product formulas (23) and (24), is comparable to 10^{-15} and is several orders of magnitude smaller than the norm of the residual using the scalar product formulas (19) and (20) in the same hydrodynamic problem.

References

1. Bahvalov N.S., Zhidkov N.P., Kobelkov G.M. *Numerical methods: a textbook for students of physics and mathematics specialties of higher educational institutions*. Binom. lab. Knowledge; 2011. 636 p. (In Russ.)

2. Ershova, T.Ya. Boundary value problem for a third-order differential equation with a strong boundary layer. *Bulletin of Moscow University. Episode 15: Computational mathematics and cybernetics*. 2020;1:30–39. (In Russ.) https://doi.org/10.3103/S0278641920010057

3. Ershova, T.Ya. On the convergence of a grid solution to the problem for a third-order equation in the case of a strong boundary layer. *Lomonosov readings: scientific conference*. Moscow: MAKS Press LLC, 2020. P. 77–78.

4. Volosova N.K. [et al.]. Modified Bubnov-Galerkin method for solving boundary value problems with a linear ordinary differential equation. *Computational Mathematics and Information Technologies*. 2024;8(3):23–33. (In Russ.) https://doi.org/10.23947/2587-8999-2024-8-3-23-33

5. Bahvalov N.S., Lapin A.V., Chizhonkov E.V. *Numerical methods in problems and exercises*. Moscow: BINOM. Knowledge laboratory; 2010. 240 p. (In Russ.)

6. Petrov A.G. High-precision numerical schemes for solving plane boundary value problems for a polyharmonic equation and their application to problems of hydrodynamics. *Applied Mathematics and Mechanics.* 2023;87(3):343–368 (In Russ.) https://doi.org/10.31857/S0032823523030128

7. Proskurin D.K., Sysoev D.V., Sazonova S.A. Convergence of the computational process when implementing the variational method for solving the boundary value problem of hydrodynamics. *Bulletin of the Voronezh State Technical University.* 2021;17(3):14–19. (In Russ) https://doi.org/10.36622/VSTU.2021.17.3.002

8. Sidoryakina V.V., Solomaha D.A. Symmetrized versions of the Seidel and upper relaxation methods for solving two-dimensional difference problems of elliptic. *Computational Mathematics and Information Technologies*. 2023;7(3):12–19. (In Russ.) https://doi.org/10.23947/2587-8999-2023-7-3-12-19

9. Alekseev V.M., Galeev E.M., Tikhomirov V.M. *Collection of optimization problems: Theory. Examples. Problems*. Moscow: Fizmatlit; 2008. 256 p. (In Russ.)

About the Authors:

Natalya K. Volosova, Post-graduate Student of Bauman Moscow State Technical University (2nd Baumanskaya St. 5–1, Moscow, 105005, Russian Federation), ORCID, navalosova@yandex.ru

Konstantin A. Volosov, Doctor of Physical and Mathematical Sciences, Professor of the Department of Applied Mathematics of the Russian University of Transport (Obraztsova St. 9–9, Moscow, GSP-4, 127994, Russian Federation), ORCID, konstantinvolosov@yandex.ru

Aleksandra K. Volosova, Candidate of Physical and Mathematical Sciences, Chief Analytical Department "Tramplin" LLC, Russian University of Transport (Obraztsova St. 9–9, Moscow, GSP-4, 127994, Russian Federation), ORCID, alya01@yandex.ru

Mikhail I. Karlov, Candidate of Physical and Mathematical Sciences, Associate Professor of the Department of Mathematics, Moscow Institute of Physics and Technology (9, Institutsky Lane, GSP-4, Dolgoprudny, 141701, Russian Federation), ORCID, karlov.mipt@gmail.com

Dmitriy F. Pastukhov, Candidate of Physical and Mathematical Sciences, Associate Professor of Polotsk State University (Blokhin St. 29, Novopolotsk, 211440, Republic of Belarus), ORCID, dmitrij.pastuhov@mail.ru

Yuriy F. Pastukhov, Candidate of Physical and Mathematical Sciences,Associate Professor of Polotsk State University (Blokhin St. 29, Novopolotsk, 211440, Republic of Belarus), ORCID, pulsar1900@mail.ru

***Contributions of the authors:* the authors contributed equally to this article.**

***Conflict of Interest Statement:* the authors declare no conflict of interest.**

All authors have read and approved the final manuscript.

Об авторах:

Наталья Константиновна Волосова, аспирант Московского государственного технического университета им. Н.Э. Баумана (105005, Российская Федерация, г. Москва, ул. 2-я Бауманская, 5, стр. 1), ORCID, navalosova@yandex.ru

Константин Александрович Волосов, доктор физико-математических наук, профессор кафедры прикладной математики Российского университета транспорта (127994, ГСП-4, Российская Федерация, г. Москва, ул. Образцова, 9, стр. 9), ORCID, konstantinvolosov@yandex.ru

Александра Константиновна Волосова, кандидат физико-математических наук, начальник аналитического отдела ООО «Трамплин» Российского университета транспорта (127994, ГСП-4, Российская Федерация, г. Москва, ул. Образцова, 9, стр. 9), ORCID, alya01@yandex.ru

Михаил Иванович Карлов, кандидат физико-математических наук, доцент кафедры математики Московского физико-технического института (141701, ГСП-4, Российская Федерация, г. Долгопрудный, Институтский переулок, 9), karlov.mipt@gmail.com

Дмитрий Феликсович Пастухов, кандидат физико-математических наук, доцент кафедры технологий программирования Полоцкого государственного университета (211440, Республика Беларусь, г. Новополоцк, ул. Блохина, 29), ORCID, dmitrij.pastuhov@mail.ru

Юрий Феликсович Пастухов, кандидат физико-математических наук, доцент кафедры технологий программирования Полоцкого государственного университета (211440, Республика Беларусь, г. Новополоцк, ул. Блохина, 29), ORCID, pulsar1900@mail.ru

Заявленный вклад авторов: **все авторы сделали эквивалентный вклад в подготовку публикации.**

Конфликт интересов: **авторы заявляют об отсутствии конфликта интересов.**

Все авторы прочитали и одобрили окончательный вариант рукописи.

Received / Поступила в редакцию 18.11.2024
Reviewed / Поступила после рецензирования 12.12.2024
Accepted / Принята к публикации 16.12.2024

INFORMATION TECHNOLOGIES
ИНФОРМАЦИОННЫЕ ТЕХНОЛОГИИ

Check for updates

UDC 004.855.5
https://doi.org/10.23947/2587-8999-2024-8-4-19-26

Original Empirical Research

Forecasting Drilling Mud Losses Using Python

Nikita V. Kornilaev[1] ✉, **Kamila F. Koledina**[1,2]
[1] Ufa State Petroleum Technological University, Ufa, Russian Federation
[2] Institute of Petrochemistry and Catalysis, Ufa Federal Research Center of the Russian Academy of Sciences, Ufa, Russian Federation
✉ nik-kornilaev@mail.ru

Abstract
Introduction. Drilling mud losses are among the most common complications encountered during well drilling. Forecasting these losses is a priority as it helps minimize drilling fluid wastage and prevent wellbore incidents. Mud loss events are primarily influenced by the geological properties of the formations being drilled. Understanding the relationship between mud loss occurrences and the geological characteristics of the formations has both fundamental and practical significance. Given the complexity of predicting mud loss probabilities using traditional mathematical models, this study aims to develop a machine-learning-based system to predict the probability of mud losses based on well location and stratigraphic description.
Materials and Methods. Experimental data from 735 wells at the Shkapovskoye oil field, including well location coordinates, geological layer indices, and mud loss intensities, were prepared for computational analysis. The dataset was divided into training and testing subsets. The classification problem was addressed using four intensity classes with the following machine learning models: Decision Tree, Random Forest, and Linear Discriminant Analysis.
Results. Predictions generated by the three models were compared against the experimental data in the test set. The evaluation metrics included accuracy and recall. All three models achieved an average prediction accuracy of 91%. Linear Discriminant Analysis was identified as the most accurate model.
Discussion and Conclusion. High-accuracy predictions enable reliable forecasting of the probability and intensity of mud losses based on the location and stratigraphic description of new wells. The study presents three machine learning methods that demonstrated superior results in solving this problem.

Keywords: Python, mud loss, drilling, machine learning methods, Decision Tree, Discriminant Analysis, Random Forest

For Citation. Kornilaev N.V., Koledina K.F. Forecasting Drilling Mud Losses Using Python. *Computational Mathematics and Information Technologies*. 2024;8(4):19–26. https://doi.org/10.23947/2587-8999-2024-8-4-19-26

Оригинальное эмпирическое исследование

Прогнозирование поглощений бурового раствора на Python

Н.В. Корнилаев[1] ✉, **К.Ф. Коледина**[1,2]
[1] Уфимский государственный нефтяной технический университет, г. Уфа, Российская Федерация
[2] Институт нефтехимии и катализа УФИЦ РАН, г. Уфа, Российская Федерация
✉ nik-kornilaev@mail.ru

Аннотация
Введение. Поглощения бурового раствора являются одним из наиболее распространённых видов осложнений в бурении скважин. Первостепенной задачей является прогнозирование процесса поглощения, так как предупреждение данного вида осложнения позволит минимизировать потери бурового раствора, а также предотвратить аварии в скважине. Возникновение поглощений обусловлено прежде всего геологическими свойствами пластов. Выяснение связи между возникновением поглощений бурового раствора и геологическими характеристиками разбуриваемых пластов представляет как фундаментальный, так и практический интерес. В

связи со сложностью определения вероятности возникновений поглощений с помощью известных математических моделей была поставлена цель исследования — построить с помощью методов машинного обучения систему, прогнозирующую значения вероятности возникновения поглощений в зависимости от местоположения скважины и её стратиграфического описания.

Материалы и методы. Экспериментальные данные о 735 скважинах Шкаповского месторождения (координаты местоположения, геологический индекс пласта, значение интенсивности поглощений) были подготовлены авторами к вычислениям. Исходные данные были разделены на обучающую и тестовую выборки. Представлены варианты решения задачи классификации по четырем классам интенсивности поглощений с использованием следующих моделей машинного обучения: «дерево решений», «случайный лес», «линейный дискриминантный анализ».

Результаты исследования. Результаты прогнозирования по трём моделям сравнивались с экспериментальными данными тестовой выборки. Для оценки качества моделей использовались метрики «точность» и «полнота». По всем трём моделям была достигнута средняя точность предсказания значений — 91 %. Было установлено, что наиболее точной моделью является «линейный дискриминантный анализ».

Обсуждение и заключение. Прогнозы высокой точности позволяют предсказывать, с какой вероятностью будут возникать поглощения определённой интенсивности в зависимости от местоположения новой скважины и её стратиграфического описания. В работе представлено три метода решения задачи, показавших наилучшие результаты.

Ключевые слова: Python, поглощение, бурение, методы машинного обучения, дерево решений, дискриминантный анализ, случайный лес

Для цитирования. Корнилаев Н.В., Коледина К.Ф. Прогнозирование поглощений бурового раствора на Python. *Computational Mathematics and Information Technologies*. 2024;8(4):19–26. https://doi.org/10.23947/2587-8999-2024-8-4-19-26

Introduction. To enhance competitiveness and optimize drilling expenses, artificial intelligence methods are widely employed in managing drilling processes today. Preventing complications and accidents remains a primary objective, as it helps minimize or entirely avoid unexpected costs associated with their mitigation.

Mud losses represent the complete or partial loss of drilling fluid as it filtrates into the formation. This phenomenon is influenced by numerous factors grouped into two major categories: geological and technological. Geological factors, such as rock properties (porosity, fracturing, permeability), have a greater impact than technological factors (properties of the selected drilling fluid, flushing fluid pressure). This is because surface operations allow for fine-tuning of the drilling process and control of critical parameters, whereas obtaining precise rock characteristics is not always feasible. Under conditions of high subsurface pressures and temperatures, formations may exhibit unpredictable properties.

In [1], the patterns of mud loss occurrences were thoroughly studied at the Yuzhno-Orlovskoye field in the Samara region. Table 1 presents data on the presence and intensity of mud losses based on research conducted at specific drilling intervals, accompanied by stratigraphic descriptions of the underlying formations.

Table 1

Intensity of Mud Losses in Wells

Well Number	Loss Interval	Stratigraphy	Mud Loss, m³/h
16	2079–2087	C_1^{t}	10
	2174–2624	$D_3^{mn} + D_3^{fm}$	catastrophic
4	2005	$D_3^{mn} + D_3^{fm}$	0.4
5	2124–2181	$D_3^{mn} + D_3^{fm}$	6–20
	2188		full
	2245–2259		
12	1925–1964	C_1^{t}	2–3
	2064–2114	D_3^{fm}	4–18
	2150–2178	D_3^{mn}	full
19	2099–2103	D_3^{fm}	12–60
	2130–2236	D_3^{mn}	full

From Table 1, it is evident that wells with similar rock properties exhibit mud losses of varying intensity, highlighting the unpredictable nature of mud loss occurrences.

Numerous studies [2–5] have focused on forecasting various types of complications and developing recommendation systems to address potential issues, including mud losses. The core of such software solutions relies on artificial neural networks trained on large volumes of geological data collected from geophysical logging stations. However, these systems share common drawbacks, including the inability to promptly obtain comprehensive downhole data in real time. This limitation restricts the amount of input data, reducing the model's prediction accuracy. Furthermore, when developing such systems, it is essential to consider the protective policies of oil and gas companies, which often make it impossible to access sufficient initial data for model development. Therefore, there is a need to create effective algorithms and software solutions capable of operating under conditions of limited input data.

The aim of this study was to develop a machine learning-based system to predict the probability of drilling mud losses of a specified intensity, depending on the well's location and the stratigraphic description of the formations being drilled.

To achieve this goal, the following tasks were undertaken:

– prepare experimental data for calculations;

– analyze machine learning algorithms and develop a program using the most optimal methods.

Materials and Methods. The Shkapovskoye oil field, located in the Republic of Bashkortostan, was selected for studying mud losses. In [6], a map of the field was presented, where wells are marked with symbols indicating the intensity of mud losses for each well. The map of the Shkapovskoye oil field is shown in Fig. 1.

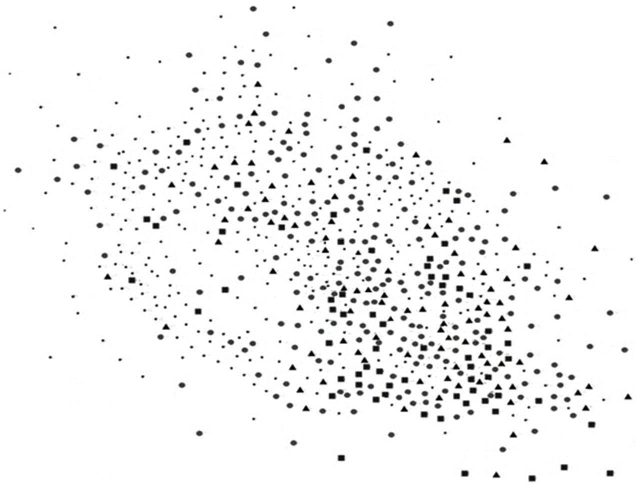

Fig. 1. Shkapovskoye Oil Field

Four classes of mud loss intensity were defined:

– 0 m³/h — no mud losses (dot, or a small circle);

– 0 to 40 m³/h — low-intensity mud losses (large circle);

– 40 to 80 m³/h — moderate-intensity mud losses (triangle);

– Over 80 m³/h — catastrophic mud losses (square).

Using the Yandex.Maps service, the length and width of the field were determined. Then, based on the map data, the coordinates of each well were calculated using the GeoGebra software package. A fragment of the calculation is shown in Fig. 2.

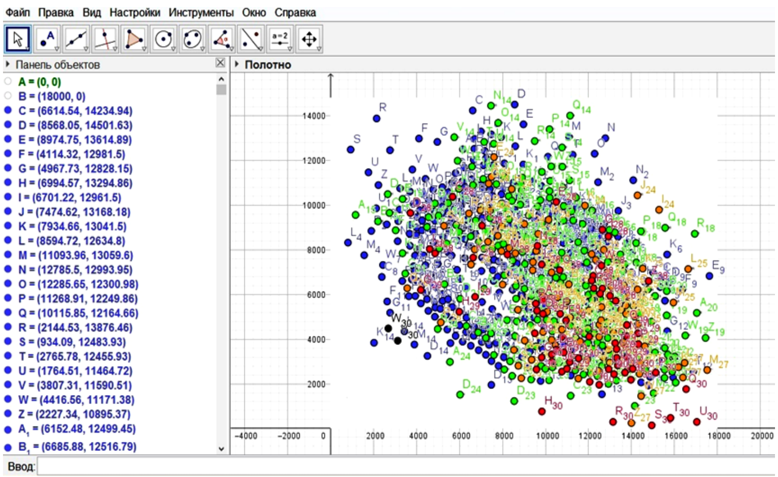

Fig. 2. Determination of Well Coordinates

Wells marked with differently colored dots correspond to mud loss intensity levels in increasing order:

– blue dots — 0 m^3/h (no mud losses);

– green dots — 0 to 40 m^3/h (low intensity);

– orange dots — 40 to 80 m^3/h (moderate intensity);

– red dots — over 80 m^3/h (catastrophic losses).

For stratigraphic descriptions, we utilized information indicating that the primary productive horizons are the Pashian (d3_p3), Kynovian (d3_kn), and Starooskolskiy (d2_st) horizons of the Devonian system. Additionally, the Bobrikovian horizon (c1_bb) has industrial significance, albeit to a lesser extent [7].

The data for the wells were categorized as follows: coordinates, stratigraphic description, and mud loss intensity. Various machine learning methods were tested on this dataset, and the most suitable ones were selected for further model optimization.

Decision Tree. This algorithm creates a tree-like structure based on "If ..., then ..." rules. These rules are generated during training on the dataset by generalizing multiple observations, making them easily interpretable. Mathematically, the decision rule can be expressed as a set of conjunctions:

$$R(x) = \wedge_{j \in J} \left[a_j \le f_i(x) \le b_j \right], \tag{1}$$

where J is the set of features selected for decision-making; $f_i(x)$ represents a real-valued feature, and a_j, b_j are the conditions. If all features satisfy the conditions, the rule returns 1; otherwise, it returns 0.

The advantages of decision trees include their simplicity of interpretation compared to neural networks and some other machine learning algorithms, as well as low requirements for data preprocessing. However, the disadvantages include a high likelihood of overfitting, as the algorithm can create excessively large trees, which may not generalize well to other datasets.

Random Forest. The Random Forest algorithm is a versatile machine learning method based on an ensemble of decision trees. Compared to other machine learning methods, the theoretical foundation of Random Forest is straightforward. The formula for the resulting classifier $a(x)$ is as follows:

$$a(x) = \frac{1}{N} \sum_{i=1}^{N} b_i(x), \tag{2}$$

where N is the number of trees; i is the tree index; b represents a decision tree, and $a(x)$ is the sample generated based on the input data.

Despite its versatility, this method has several significant drawbacks:

– difficulty in interpretation;

– inability to extrapolate;

– susceptibility to overfitting on highly noisy data;

– bias towards features with a larger number of levels when working with datasets containing categorical variables with varying levels [9].

Linear Discriminant Analysis (LDA). The main idea behind the selected algorithm is based on the assumption of a multivariate normal distribution within classes and the search for a linear transformation that maximizes the between-class variance while minimizing the within-class variance [10].

The proposed algorithm has the following advantages:

– lower tendency to overfit (compared to logistic regression), as LDA models the data distribution within each class and requires fewer parameters for estimation;

– it is more stable and efficient when there is a large number of classes with good linear separability.

The main disadvantage of LDA is its sensitivity to outliers and inefficiency when the number of features significantly exceeds the number of objects.

Results. The classification task was solved using the Python programming language, with the libraries sklearn, pandas, numpy, tkinter, and the MySQL DBMS. The program flowchart is shown in Fig. 3.

To visualize the modeling results, we compared the absorption intensity of wells in the test sample with the absorption intensities predicted by the models. The absorption intensity schemes for the test sample wells are shown in Fig. 4.

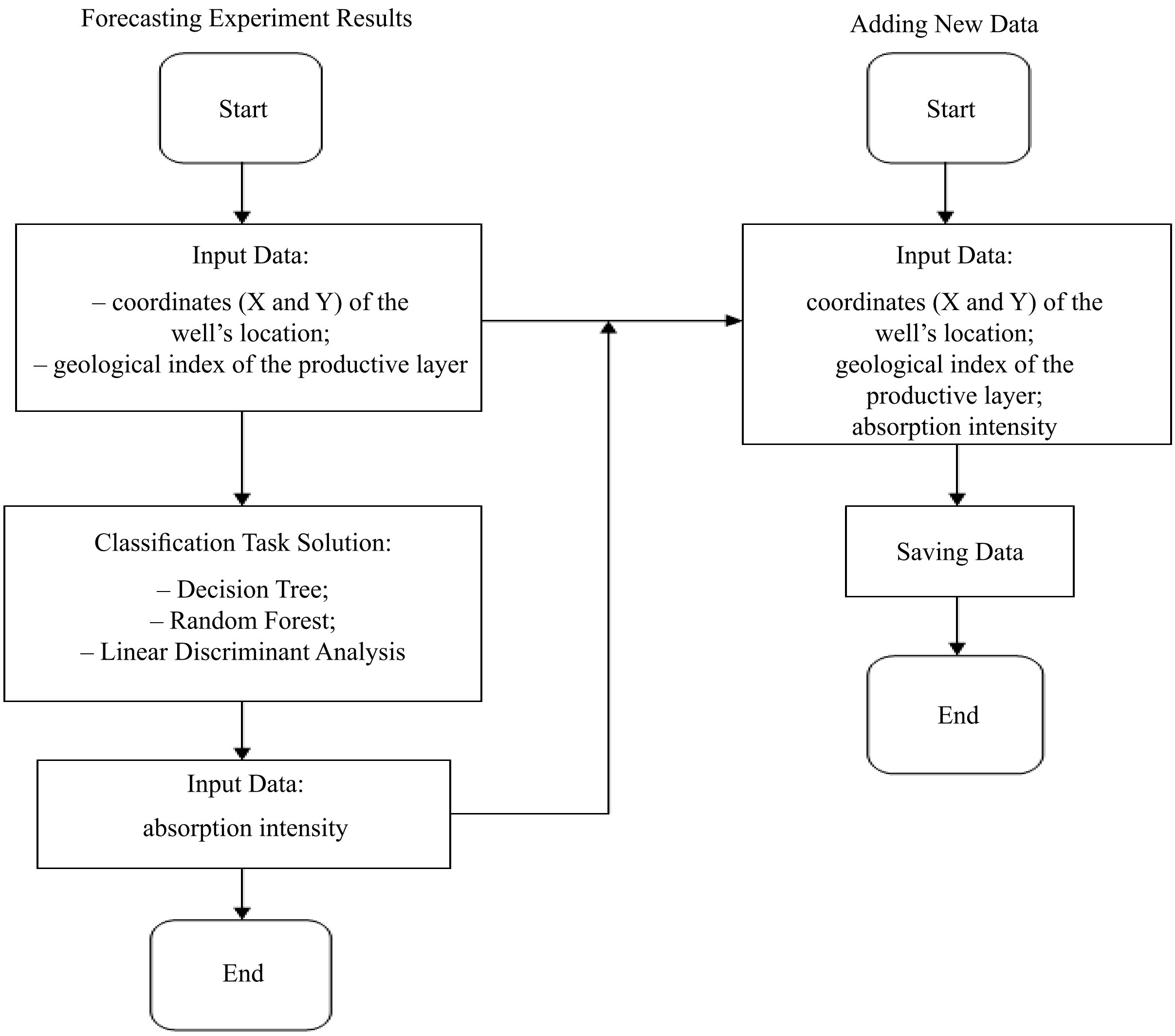

Fig. 3. The program flowchart

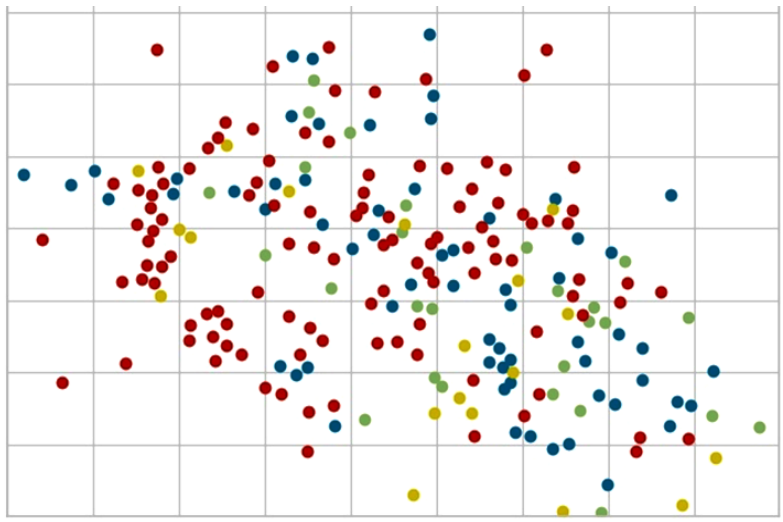

Fig. 4. Absorption intensity scheme (test sample wells)

Wells marked with differently colored dots correspond to mud loss intensity levels in increasing order:
– blue dots — 0 m³/h (no mud losses);
– green dots — 0 to 40 m³/h (low intensity);
– orange dots — 40 to 80 m³/h (moderate intensity);

– red dots — over 80 m³/h (catastrophic losses).

Fig. 5–7 show the schemes of the deposits with wells and predicted absorption intensities for the three machine learning models considered. Differences from the test sample are noted.

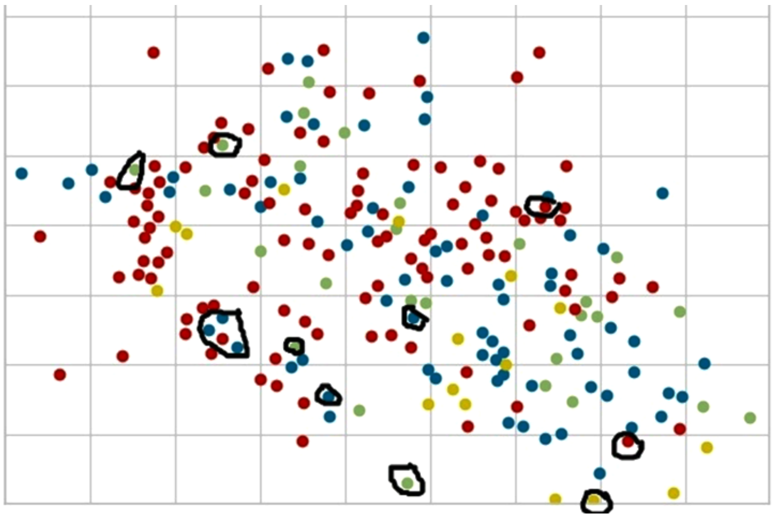

Fig. 5. Absorption intensity scheme (for the "Decision Tree" algorithm)

Wells marked with differently colored dots correspond to mud loss intensity levels in increasing order:
– blue dots — 0 m³/h (no mud losses);
– green dots — 0 to 40 m³/h (low intensity);
– orange dots — 40 to 80 m³/h (moderate intensity);
– red dots — over 80 m³/h (catastrophic losses).

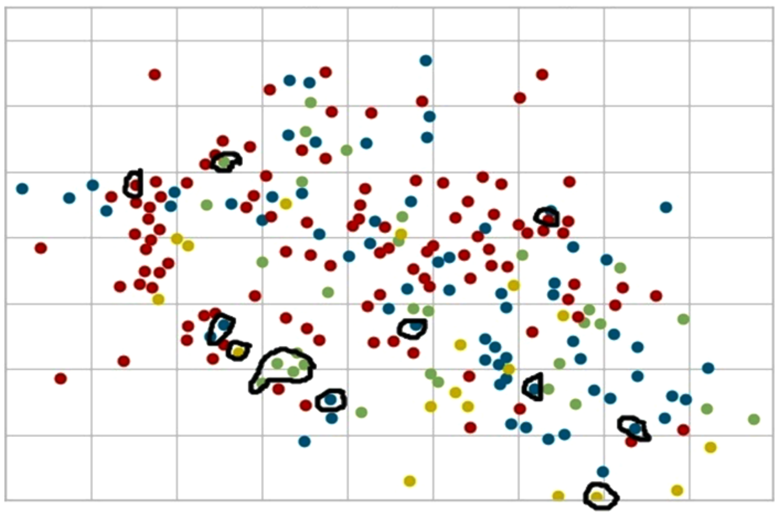

Fig. 6. Absorption intensity scheme (for the "Linear Discriminant Analysis" algorithm)

Wells marked with differently colored dots correspond to mud loss intensity levels in increasing order:
– blue dots — 0 m³/h (no mud losses);
– green dots — 0 to 40 m³/h (low intensity);
– orange dots — 40 to 80 m³/h (moderate intensity);
– red dots — over 80 m³/h (catastrophic losses).

The greatest number of "mismatches" was observed with the "Random Forest" algorithm model. This can be explained by the insufficient size and number of features in the training sample for constructing the ensemble of decision trees.

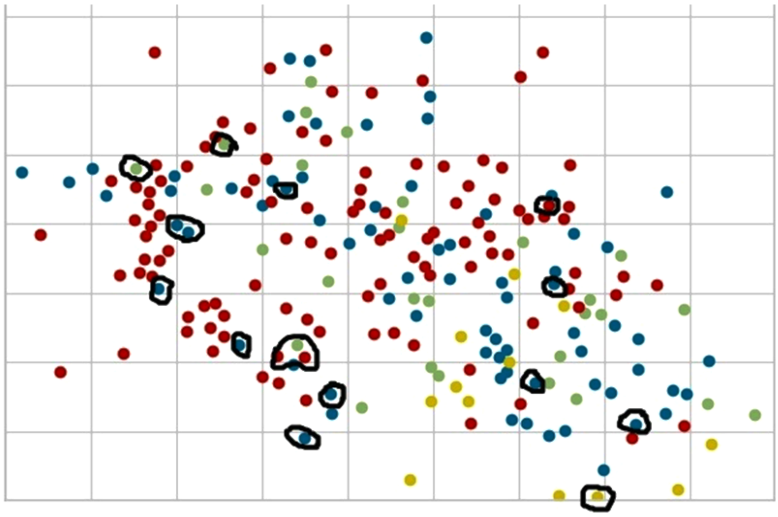

Fig. 7. Absorption intensity scheme (for the “Random Forest” algorithm)

For accuracy metrics, recall (sensitivity) was used, which characterizes the ability to identify the considered class, as well as precision, which allows distinguishing one class from another. These metrics are calculated using formulas (3, 4):

$$\text{precision} = \frac{TP}{TP + FP}, \tag{3}$$

$$\text{recall} = \frac{TP}{TP + FN}, \tag{4}$$

where TP — True Positives: correctly predicted values of the class under consideration; FP — False Positives: incorrectly predicted values of the class under consideration; FN — False Negatives: incorrectly predicted values of other classes.

The calculation results for each class are presented in Table 2.

Table 2

Metrics for evaluating the quality of machine learning models

Absorption Class	Precision max	Recall max
0 m^3	0.88 (LDA)	0.97 (Decision Tree)
0–40 m^3	0.89 (Random Forest)	0.93 (LDA)
40–80 m^3	0.93 (Decision Tree)	0.84 (LDA)
> 80 m^3	0.98 (LDA)	0.92 (Random Forest)

From Table 2, it can be concluded that all three models demonstrated high prediction performance. The most effective algorithm for the problem at hand is Linear Discriminant Analysis.

Discussion and Conclusion. The results obtained during the prediction of drilling fluid loss intensity in wells are relevant for practical application in assessing complications in the field. Despite the high predictive capability of the model, its main limitation is the lack of applicability to other fields. To achieve accurate classification for different fields, the model must be retrained on the corresponding operational data.

Thus, it is essential to develop solutions for the preliminary analysis of “raw” data provided by geological exploration and the subsequent transfer of processed data to machine learning algorithms.

References

1. Shipovskiy K.A., Tsirkova V.S., Koval M.E., Kozhin V.N. Regularities of the distribution of lost circulation areas in single reefs of the depression zone of the Kama-Kinel downfold system. *Exposition Oil & Gas*. 2021;1(80):34–39. (In Russ.) https://doi.org/10.24412/2076-6785-2021-1-34-39

2. Eremin N.A., Selenginsky D.A. On the possibilities of applying artificial intelligence methods in solving oil and gas problems. *Proceedings of Tula State University. Earth sciences*. 2023;1(1):201–211. (In Russ.) https://doi.org/10.46689/2218-5194-2023-1-1-201-211

3. Abu-Abed F.N., Borisov N.A., Khabarov A.R. The use of pattern recognition methods for the analysis of emergency situations. In: *Collection of articles of the XVI International scientific and practical conference "Mathematical methods and information technologies in economics, Sociology and Education"*. Penza: Autonomous non-profit scientific and educational organization "Volga House of Knowledge"; 2005. pp. 428–431. (In Russ.)

4. Kodirov Sh.Sh., Shestakov A.L. Development of an artificial neural network for predicting the tack of drill pipe columns. *Bulletin of SUSU. The series "Computer technology, control, radio electronics"*. 2019;19(3):20–32. (In Russ.) https://doi.org/10.14529/ctcr190302

5. Dmitrievsky A.N., Eremin N.A., Chernikov A.D., Zinatulina L.I. The use of artificial intelligence methods to prevent complications during well construction. *Proceedings of Tula State University. Earth sciences*. 2021;4:132–145. (In Russ.) https://doi.org/10.46689/2218-5194-2021-4-1-132-144

6. Lind Yu.B., Kabirova A.R., Nurislamova L.F. Predicting complications in the drilling process using parallel computing technology. In: *Proceedings of the international scientific conference "Parallel Computing Technologies"*. Novosibirsk: SUSU Publishing Center; 2012. pp. 571–576. (In Russ.)

7. Trebin G.F., Charygin N.V., Obukhova T.M. *Oil fields of the Soviet Union. Guide*. 2nd ed., additional and revised. Moscow: Nedra; 1980. 583 p. (In Russ.)

8. DecisionTrees — Geeksforgeeks. URL: https://www.geeksforgeeks.org/decision-tree-introduction-example/ (accessed: 21.04.2024).

9. Random Forest Algorithm in Machine Learning — Geekforgeeks. URL: https://www.geeksforgeeks.org/random-forest-algorithm-in-machine-learning/ (accessed: 21.04.2024).

10. Linear Discriminant Analysis in Machine Learning — GeeksforGeeks. URL: https://www.geeksforgeeks.org/ml-linear-discriminant-analysis/ (accessed: 21.04.2024).

About the Authors:

Nikita V. Kornilaev, student at the Department of Information Technologies and Applied Mathematics of the Ufa State Petroleum Technological University (1, Kosmonavtov str., Ufa, 450064, Russian Federation), ORCID, nik-kornilaev@mail.ru

Kamila F. Koledina, Dr. Sc. (Phys.-Math.), Associate Professor at the Department of Information Technologies and Applied Mathematics of the Ufa State Petroleum Technological University (1, Kosmonavtov str., 450064, Ufa, Russian Federation), Research Fellow of the Institute of Petrochemistry and Catalysis of the Russian Academy of Sciences (450075, October ave., 141, Ufa, Russian Federation), ORCID, koledinakamila@mail.ru

Claimed Contributorship:

N.V. Kornilaev: Program development and algorithm implementation.

K.F. Koledina: task formalization, testing, specification development.

Conflict of Interest Statement: **the authors declare no conflict of interest.**

All authors have read and approved the final manuscript.

Об авторах:

Никита Владимирович Корнилаев, студент кафедры информационных технологий и прикладной математики Уфимского государственного нефтяного технологического университета (450064, Российская Федерация, г. Уфа, ул. Космонавтов, 1), ORCID, nik-kornilaev@mail.ru

Камила Феликсовна Коледина, доктор физико-математических наук, доцент кафедры информационных технологий и прикладной математики Уфимского государственного нефтяного технологического университета (450064, Российская Федерация, г. Уфа, ул. Космонавтов, 1), научный сотрудник Института нефтехимии и катализа Российской академии наук (450075, Российская Федерация, г. Уфа, пр-т Октября, 141), ORCID, koledinakamila@mail.ru

Заявленный вклад авторов:

Н.В. Корнилаев: разработка программы и реализация алгоритма.

К.Ф. Коледина: формализация задачи, тестирование, разработка спецификации.

Конфликт интересов: **авторы заявляют об отсутствии конфликта интересов.**

Все авторы прочитали и одобрили окончательный вариант рукописи.

Received / Поступила в редакцию 21.10.2024

Reviewed / Поступила после рецензирования 07.11.2024

Accepted / Принята к публикации 15.11.2024

INFORMATION TECHNOLOGIES
ИНФОРМАЦИОННЫЕ ТЕХНОЛОГИИ

UDC 519.6

https://doi.org/10.23947/2587-8999-2024-8-4-27-34

Original Theoretical Research

Forecasting the Dynamics of Summer Phytoplankton Species based on Satellite Data Assimilation Methods

Yulia V. Belova[1] ✉, Alena A. Filina[2], Alexander E. Chistyakov[1]

[1] Don State Technical University, Rostov-on-Don, Russian Federation

[2] Supercomputers and Neurocomputers Research Center, Taganrog, Russian Federation

✉ yvbelova@yandex.ru

Abstract

Introduction. Mathematical tools integrated with satellite data are typically employed as the primary means for studying aquatic ecosystems and forecasting changes in phytoplankton concentration in shallow water bodies during summer. This approach facilitates accurate monitoring, analysis, and modelling of the spatiotemporal dynamics of biogeochemical processes, considering the combined effects of various physicochemical, biological, and anthropogenic factors impacting the aquatic ecosystem. The authors have developed a mathematical model aligned with satellite data to predict the behavior of summer phytoplankton species in shallow water under accelerated temporal conditions. The model describes oxidative-reduction processes, sulfate reduction, and nutrient transformations (phytoplankton mineral nutrition), investigates hypoxia events caused by anthropogenic eutrophication, and forecasts changes in the oxygen and nutrient regimes of the water body.

Materials and Methods. To simulate the population dynamics of summer phytoplankton species correlated with satellite data assimilation methods, an operational algorithm for restoring water quality parameters of the Azov Sea was developed based on the Levenberg-Marquardt multidimensional optimization method. The initial distribution of phytoplankton populations was obtained by applying the Local Binary Patterns (LBP) method to satellite images of the Taganrog Bay and was used as input data for the mathematical model.

Results. Using integrated hydrodynamic and biological kinetics models combined with satellite data assimilation methods, a software suite was developed. This suite enables short- and medium-term forecasts of the ecological state of shallow water bodies based on diverse input data correlated with satellite information.

Discussion and Conclusion. The conducted studies on aquatic systems revealed that improving the accuracy of initial data is one mechanism for enhancing the quality of biogeochemical process forecasting in marine ecosystems. It was established that using satellite data alongside mathematical modeling methods allows for studying the spatiotemporal distribution of pollutants of various origins, plankton populations in the studied water body, and assessing the nature and scale of natural or anthropogenic phenomena to prevent negative economic and social consequences.

Keywords: forecasting, summer phytoplankton populations, coastal system, satellite data, numerical experiment

Funding. The study was supported by the Russian Science Foundation grant no. 22–71–10102, https://rscf.ru/project/22-71-10102/

For Citation. Belova Yu.V., Filina A.A., Chistyakov A.E. Forecasting the dynamics of summer phytoplankton species based on satellite Data assimilation methods. *Computational Mathematics and Information Technologies*. 2024;8(4): 27–34. https://doi.org/10.23947/2587-8999-2024-8-4-27-34

Оригинальное теоретическое исследование

Прогнозирование динамики летних видов фитопланктона на основе методов усвоения спутниковых данных

Ю.В. Белова[1] ✉, А.А. Филина[2], А.Е. Чистяков[1]

[1] Донской государственный технический университет, г. Ростов-на-Дону, Российская Федерация

[2] ООО «НИЦ супер-ЭВМ и нейрокомпьютеров», г. Таганрог, Российская Федерация

✉ yvbelova@yandex.ru

Аннотация

Введение. В качестве основного инструмента исследований функционирования водных экосистем и прогнозирования изменения концентрации фитопланктона в мелководном водоеме в летний период обычно используется математический инструментарий с применением спутниковых данных, что позволяет осуществлять корректный мониторинг, анализ и моделирование динамики протекания биогеохимических процессов в пространстве и во времени с учетом совокупного действия ряда физико-химических, биологических и антропогенных факторов, влияющих на изучаемую водную экосистему. Авторами разработана математическая модель, коррелирующая со спутниковой информацией, позволяющая прогнозировать поведение летних видов фитопланктона в мелководном водоеме в условиях ускоренного времени, описывать окислительно-восстановительные процессы водной среды, сульфатредукции, трансформации биогенных веществ (минерального питания фитопланктона), изучать развитие заморных явлений, возникающих в результате антропогенной эвтрофикации, строить прогнозы изменения кислородного и биогенного режимов функционирования водоема.

Материалы и методы. Для моделирования численности видового состава летнего фитопланктона, коррелирующего с методами усвоения спутниковых данных, разработан оперативный алгоритм восстановления параметров качества вод Азовского моря, который базируется на методе многомерной оптимизации Левенберга-Марквардта. Начальное распределение фитопланктонных популяций было получено в результате применения метода LBP (локальных бинарных шаблонов) к космическим снимкам Таганрогского залива и использовано в качестве входных данных для разработанной математической модели.

Результаты исследования. На основе скомплексированных моделей гидродинамики и биологической кинетики, а также методов усвоения спутниковых данных, разработан программный комплекс, который позволяет строить кратко- и среднесрочные прогнозы экологической обстановки мелководных водоемов на основе различных входных данных, коррелирующих со спутниковой информацией.

Обсуждение и заключение. В рамках проводимых исследований состояния водных систем установлено, что одним из механизмов повышения качества прогнозирования биогеохимических процессов морских экосистем является уточнение начальных данных. Установлено, что использование спутниковых данных наряду с методами математического моделирования позволяют изучать пространственно-временное распределение загрязнений различной природы, планктонных популяций исследуемого водного объекта, оценивать характер и масштабы природного или техногенного явления для предотвращения негативных последствий экономического и социального характера.

Ключевые слова: прогнозирование, популяции летнего фитопланктона, прибрежная система, спутниковые данные, численный эксперимент

Финансирование. Исследование выполнено за счет гранта Российского научного фонда № 22–71–10102, https://rscf.ru/project/22-71-10102/

Для цитирования. Белова Ю.В., Филина А.А., Чистяков А.Е. Прогнозирование динамики летних видов фитопланктона на основе методов усвоения спутниковых данных. *Computational Mathematics and Information Technologies*. 2024;8(4):27–34. https://doi.org/10.23947/2587-8999-2024-8-4-27-34

Introduction. Remote sensing of the Earth (RSE) represents a modern and promising method for assessing the biological state of shallow water bodies, as well as the dynamics of biogeochemical processes, including the behavior of phytoplankton populations during the summer in shallow aquatic systems. A key challenge in this domain is developing and implementing computationally efficient forecasting algorithms and providing them with real-world input data. Addressing this challenge is fundamental to solving numerical modelling problems in hydrobiology for water bodies in southern Russia.

Research in this field is actively conducted by both Russian and international scientists. For example, [1] describes the application of remote sensing methods to map cyanobacterial blooms in lakes in northern Italy. The study in [2] demonstrates the effectiveness of the Maximum Peak Height (MPH) algorithm of MERIS in extracting chlorophyll-a (chl-a) concentrations as a tool for monitoring water body eutrophication. G.I. Marchuk, V.P. Shutyaev, G.K. Korotaev, and V.B. Zalesny have significantly contributed to data assimilation methods in atmospheric and ocean physics problems [3, 4]. A.A. Zelenko and Yu.D. Resnyansky have studied marine observation systems [5]. O.I. Krivorotko and S.I. Kabanikhin developed algorithms for reconstructing disturbance sources in the nonlinear shallow water equations system [6].

The works of G.I. Marchuk and V.P. Shutyaev focus on iterative algorithms based on the theory of adjoint equations, allowing the solution of variational data assimilation problems [7]. Y. Chao, H. Zhang, et al., in [8], proposed a three-dimensional ocean modelling system for the California region that processes satellite data in real time. This ocean model features a horizontal resolution of approximately three kilometers and employs a multi-scale three-dimensional variational data assimilation methodology.

In [9], researchers Robertson R. and Dong C. compare several vertical mixing parameterization algorithms for oceanic waters: modifications of the Nakanishi-Niino Mellor-Yamada algorithm (NN), the Large-McWilliams-Doney's Kpp algorithm (LMD), Mellor-Yamada 2.5 (MY), and four versions of the Generic Length Scale (GLS) algorithm. Algorithms for processing satellite images to parameterize hydrodynamic and hydrobiological models and identify pollution zones are also actively developed. Study [10] describes algorithms and provides code for automatic detection of upwelling filaments (AFD) based on image processing and pattern recognition. Study [11] explores the potential use of Sentinel-2 satellite images with unmanned aerial vehicles for obtaining multispectral aerial photographs to detect marine surface debris for monitoring, collection, and removal.

The aim of this study is to integrate effective mathematical modeling methods with satellite data assimilation techniques to conduct detailed investigations into the functioning of aquatic ecosystems and forecast the dynamics of summer phytoplankton population changes in shallow water bodies. This approach enables the observation and analysis of the spatiotemporal dynamics of biogeochemical processes in shallow systems while accounting for the combined influence of physicochemical, biological, and anthropogenic factors affecting the studied aquatic ecosystem.

Materials and Methods. The developed 4D mathematical model of summer phytoplankton evolution in coastal systems is based on a system of unsteady partial differential equations with nonlinear source terms ψ_i:

$$\frac{\partial q_i}{\partial t}+u\frac{\partial q_i}{\partial x}+v\frac{\partial q_i}{\partial y}+\left(w-w_{gi}\right)\frac{\partial q_i}{\partial z}=\mu_i\Delta q_i+\frac{\partial}{\partial z}\left(\nu_i\frac{\partial q_i}{\partial z}\right)+\psi_i, \tag{1}$$

where u, v, w are the components of the velocity vector for convective transport; μ_i, ν_i are the coefficients of turbulent transport in the horizontal and vertical directions, respectively; w_{gi} is the gravitational settling velocity of the i-th component in suspension; Δ is the two-dimensional Laplace operator; ψ_i are nonlinear source functions describing chemical and biological processes; i is the type of substance, $i \in M = \{P, MP, N, D, BT, BD, H_2S, S, SO_4, O_2\}$. The set of modeled substances is detailed in Table 1.

Table 1

Set of Modeled Substances

No.	Symbol	Description
1	P	Summer phytoplankton species
2	MP	Phytoplankton metabolite
3	N	Nutrients
4	D	Detritus
5	BT	Aerobic bacteria *Thiobacillus*
6	BD	Anaerobic bacteria *Desulfovibrio*
7	H_2S	Hydrogen sulfide
8	S	Elemental sulfur
9	SO_4	Sulfates
10	O_2	Dissolved oxygen

The source functions and model parameters are described in detail in [12]. Appropriate initial and boundary conditions are incorporated into the model.

The presented mathematical model builds upon the foundational works of prominent researchers, including A.I. Sukhinov, B.N. Chetverushkin, G.G. Matishov, E.V. Yakushev, and E.R. Weiner, among others [13, 14].

Development of a Software Suite for Research and Forecasting. The forecasting of phytoplankton dynamics in a shallow waterbody during the summer period was carried out using the developed research and forecasting complex (RFC), equipped with an integrable algorithm for interaction with geographic information systems (GIS). The software and algorithmic framework is designed to analyze and evaluate the scale of natural disasters (including eutrophication, “blooming”, pollution by components of various etiologies, etc.) and to generate short- and medium-term forecasts of their development in accelerated time frames, with the potential for mitigating economic and social impacts.

Given the rapid escalation of factors adversely affecting the progression of hazardous and emergency events (climatic and anthropogenic), the use of modern and efficient forecasting methodologies integrated with GIS and satellite data is highly relevant today.

Modelling the dynamics of biological and geochemical indicators of the shallow waterbody (the Azov Sea and the Taganrog Bay) was carried out by solving direct and inverse remote sensing (RS) problems for aquatic environments. The solution to the direct problem of remote sensing in the visible range involves determining the spectral dependence of the reflection coefficient $R_{rsw} = (\lambda,–0,\theta_0, \beta)$ as a function of the concentrations of water system components and their optical properties [15]:

$$R_{rsw}\left(\lambda,-0,\theta_0,\beta\right)= T_{surf} L_w\left(+0,\theta_v,\beta_v,\lambda\right)/E_d\left(+0,\lambda\right), \tag{8}$$

where λ is the wavelength; β is the viewing angle of the water surface by the satellite sensor; θ_0 is the solar zenith angle; T_{surf} is the solar light attenuation factor when passing through the “water-air” interface; $E_d(+0,\lambda)$ is the illumination of the water surface, and $L_w(+0,\theta_v,\beta_v,\lambda)$ is the brightness of the water surface, determined using remote sensing data.

The solution to the inverse problem is based on developing an algorithm for retrieving water parameters from satellite data. Optical properties of water are influenced by living organisms, dissolved and suspended substances, micro-turbulent inhomogeneities, and bubble gases. This study highlights the primary color-forming components (water, dissolved organic matter (DOM); chlorophyll from phytoplankton (Chl), and mineral suspension (MS)), as well as the primary hydro-optical water parameters (a — absorption coefficient; b_b — backscattering coefficient). These parameters are convolutions of the optical properties of the color-forming components, characterized by additive properties:

$$a=\sum_{k=1}^{K} C_k a_k^*;\quad b=\sum_{k=1}^{K} C_k b_{bk}^*, \tag{9}$$

where a_k^*, b_{bk}^* are the primary hydro-optical characteristics of the k-th component; C_k is the specific concentration of the k-th component. The set of spectral values of the a^*, b_b^* coefficients constitutes the hydro-optical model of the Azov Sea. The coefficient $R_{rsw} = (\lambda,–0,\theta_0, \beta)$ is determined as a secondary hydro-optical characteristic of the aquatic environment, describing water properties and brightness characteristics. It is calculated at the horizon based on the surface layer of the water column and shows minimal dependency on θ_0 and β:

$$R_{rsw}\left(\lambda,\mathbf{C},a,b_b\right)=a_0+a_1\left\{b_b\left(\lambda\right)/a\left(\lambda\right)\right\}+a_2\left\{b_b\left(\lambda\right)/a\left(\lambda\right)\right\}^2, \tag{10}$$

where $a_k, k=\overline{0,2}$, $b_b(\lambda)$, $a(\lambda)$ are the known coefficients for each component of the aquatic environment (hydro-optical model of the Azov Sea).

Let us describe the developed algorithm for retrieving water parameters of the Azov Sea, which is based on the efficient Levenberg-Marquardt (LM) multidimensional optimization method. The concentration vector of color-forming components was represented as:

$$\mathbf{C}=\left(C_{хл},C_{мв},C_{ров}\right)^{\tau}.$$

To find the optimal concentration vector **C** an absolute minimum of the residual function $f(\mathbf{C})$ was sought:

$$f\left(\mathbf{C}\right)=\sum_j\left[S_j-R_{rsw}\left(\lambda,\mathbf{C},a,b_b\right)\right]^2. \tag{11}$$

The expression for calculating the optimal vector **C** is as follows:

$$\mathbf{C}_{k+1}=\mathbf{C}_k+\lambda_k\left(F_k^{\tau}F_k+\mu_k D_k\right)^{-1}F_k R_{rsw}\left(\lambda,\mathbf{C}_k,a,b_b\right), \tag{12}$$

where $F_k=\left(\dfrac{\partial R_{rsw}\left(\lambda,\mathbf{C}_k,a,b_b\right)}{\partial \mathbf{C}_k}\right)$ is the matrix; μ_k is the direction of minimization; D_k is the diagonal of the matrix $F_k^{\tau}F$; λ_k is the step size of the optimization; τ denotes the transpose operation.

Expressions (9) and the parameterization in (10) were used to calculate the spectral value of the reflectance coefficient of the water column based on the concentration vectors of color-forming components. Calculations were performed for the wavelengths 412, 443, 490, 510, 590, and 670 nm (corresponding to the Sea Viewing Wide Field Sensor (SeaWiFS) channels).

In addition to synchronous remote sensing data from SeaWiFS sensors and the MODIS spectrometer, in situ measurements of hydrodynamic, hydro-optical, and biogeochemical parameters of the studied water body were used to verify the accuracy of the retrieved vector CoptC_{\text{opt}}Copt obtained using the LM algorithm. These measurements included scattering, absorption, and attenuation coefficients for nine wavelengths in the spectral range of 412–715 nm, collected at each station during field expeditions.

A comparison of the measured and retrieved concentrations of color-forming components from satellite monitoring data showed agreement, with a correlation coefficient averaging 0.75.

Results. A computational experiment was conducted based on integrated hydrodynamic and biological kinetics models. The Taganrog Bay was chosen as the real modelling area since this part of the Azov Sea produces the majority of phytoplankton biomass during the summer. A module for calculating biological kinetics processes was developed and integrated into the “Azov3D” software suite [16–18].

The input data for the calculations included salinity and temperature distributions derived from cartographic information, water flow velocity calculated using a hydrodynamic mathematical model, and processed long-term observational data on the concentrations of nutrients and key phytoplankton species [19]. Additionally, the spatial distribution of phytoplankton populations, obtained using the Local Binary Patterns (LBP) method applied to satellite images, was used as input data. The method was developed by the authors of this research [20].

The LBP method enables the detection of the boundaries of phytoplankton “blooms” and pollutants, including oil and petroleum products, in satellite images. Figure 1 *a* shows the initial satellite image captured on August 6, 2020, by the Sentinel-2 L2A satellite [21]. Figure 1 *b* presents the initial distribution of phytoplankton populations, derived using the LBP method, which serves as input data for the program module. The concentration values reflect typical summer phytoplankton levels based on long-term observations.

The results of the software suite’s operation for a 30-day time interval and uniform initial distributions of phytoplankton and nutrient substances are shown in Figure 2.

a)

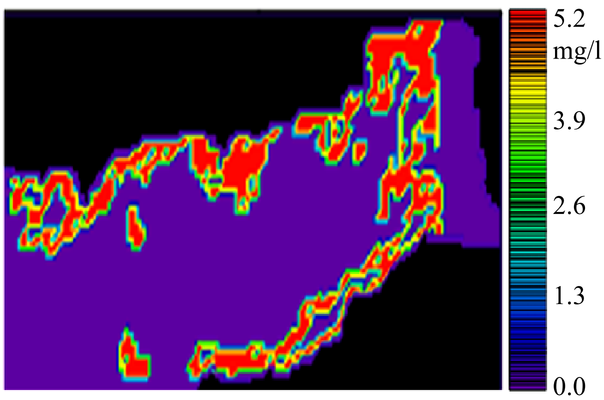

b)

Fig. 1. Phytoplankton Images
a — Satellite image of the modeled area;
b — Initial distribution of phytoplankton populations

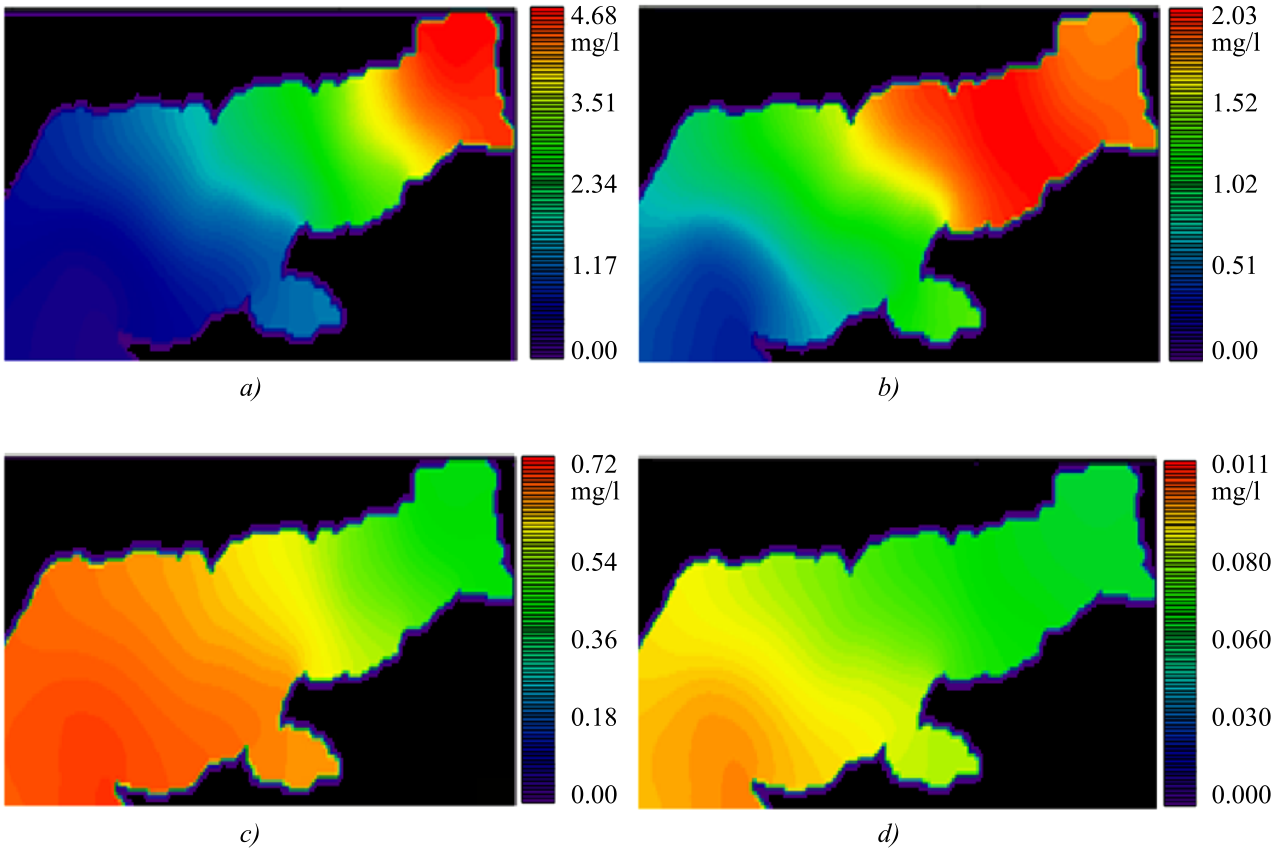

Fig. 2. Distribution of Concentrations in Taganrog Bay During the Summer Period
a — Chlorella vulgaris green algae; *b* — Aphanizomenon flos-aquae cyanobacteria; *c* — Phosphates; *d* — Nitrates

Discussion and Conclusion. The research on the state of aquatic systems has revealed that one of the mechanisms for improving the quality of biogeochemical process forecasting in marine ecosystems is refining initial data. In data assimilation systems, alongside stationary measurements, methods for processing and assimilating satellite information, which have been actively developed in the country over the past decades, have gained significant importance. It has been established that using satellite data in conjunction with mathematical modelling methods enables the study of the spatiotemporal distribution of various pollutants and plankton populations in the studied water body. This approach also helps assess the nature and scale of natural or anthropogenic events to prevent adverse economic and social impacts.

The authors have developed a spatially heterogeneous mathematical model of summer phytoplankton evolution in a shallow water body, numerically implemented in a research and forecasting complex (RFC). This complex integrates with various GIS platforms and satellite data. The model provides real-time forecasting of changes in density and spatial distribution of plankton populations. It also facilitates the study and analysis of redox processes, the transformation of nutrients (mineral feeding of phytoplankton), and sulfate reduction occurring within the water column. Additionally, the model examines the development of fish-kill events caused by anthropogenic eutrophication and predicts changes in the oxygen and nutrient regimes of the water body.

The RFC enables the development of comprehensive preventive measures to ensure environmental safety and mitigate economic damage in the studied region. The study also constructed an efficient and rapid algorithm for restoring water parameters in the shallow region (Azov Sea), based on the effective Levenberg-Marquardt multidimensional optimization method.

The developed RFC can be effectively applied to generate short- and medium-term environmental forecasts for shallow water bodies in Southern Russia. It utilizes diverse input information, such as the spatial distribution of phytoplankton during the summer period, obtained using the Local Binary Patterns method applied to satellite imagery.

References

1. Bresciani M., Giardino C., Lauceri R., Matta E., Cazzaniga I., Pinardi M., et al. Earth observation for monitoring and mapping of cyanobacteria blooms. Case studies on five Italian lakes. *Journal of Limnology*. 2017;76:127–139. https://doi.org/10.4081/jlimnol.2016.1565

2. Pitarch J., Ruiz-Verdú A., Sendra M.D., and Santoleri R. Evaluation and reformulation of the maximum peak height algorithm (MPH) and application in a hypertrophic lagoon. *Journal of Geophysical Research: Oceans*. 2017;122(2):1206–1221. https://doi.org/10.1002/2016JC012174

3. Shutyaev V.P. Methods for observation data assimilation in problems of physics of atmosphere and ocean. *Izvestiya, Atmospheric and Oceanic Physics*. 2019;55(1):17–31. https://doi.org/10.1134/S0001433819010080

4. Korotaev G.K., Shutyaev V.P. Numerical simulation of ocean circulation with ultrahigh spatial resolution. *Proceedings of the Russian Academy of Sciences. Physics of the atmosphere and ocean*. 2020;56(3):334–346. (In Russ.) https://doi.org/10.31857/S0002351520030104

5. Zelenko A.A., Resnyansky Yu.D. Marine observation systems as an integral part of operational oceanology (review). *Meteorology and hydrology*. 2018;12:5–30. (In Russ.)

6. Kabanikhin S.I., Krivorotko O.I. Algorithm for restoring the source of disturbances in a system of nonlinear shallow water equations. *Journal of Computational Mathematics and Mathematical Physics*. 2018;58(8):138–147. (In Russ.) https://doi.org/10.31857/S004446690002008-9

7. Marchuk G.I., Shutyaev V.P. Conjugate equations and iterative algorithms in problems of variational data assimilation. *Proceedings of the Institute of Mathematics and Mechanics of the Ural Branch of the Russian Academy of Sciences*. 2011;17(2):136–150. (In Russ.)

8. Chao Y., Farrara J.D., Zhang H., Armenta K.J., Centurioni L., Chavez F., et al. Development, Implementation, and Validation of a California Coastal Ocean Modeling, Data Assimilation, and Forecasting System. *Deep-Sea Research Part II: Topical Studies in Oceanography*. 2018;151:49–63. https://doi.org/10.1016/j.dsr2.2017.04.013

9. Robertson R., Dong C. An evaluation of the performance of vertical mixing parameteriza-tions for tidal mixing in the Regional Ocean Modeling System (ROMS). *Geoscience Letters*. 2019;6(15). https://doi.org/10.1186/s40562-019-0146-y

10. Artal O., Sepúlveda H.H., Mery D., Pieringer C. Detecting and characterizing upwelling filaments in a numerical ocean model. *Computers and Geosciences.* 2019;122:25–34. https://doi.org/10.1016/j.cageo.2018.10.005

11. Themistocleous K., Papoutsa C., Michaelides S., Hadjimitsis D. Investigating Detection of Floating Plastic Litter from Space Using Sentinel-2 Imagery. *Remote Sensing*. 2020;12(16):2648. https://doi.org/10.3390/RS12162648

12. Nikitina A.V., Filina A.A. Mathematical modeling of the processes of evolution of microorganisms in a shallow reservoir in oxygen-deficient conditions. Intelligent information technologies and mathematical modeling. *Proceedings of the International Scientific Conference*. Edited by V.V. Dolgov. Rostov-on-Don. 2022:66–75. (In Russ.)

13. Chetverushkin B.N. Resolution limits of continuous media mode and their mathematical formulations. *Math Models Comput Simul*. 2013;5:266–279. https://doi.org/10.1134/S2070048213030034

14. Yakushev E.V., Mikhailovsky G.E. Mathematical modeling of the influence of marine biota on the carbon dioxide ocean-atmosphere exchange in high latitudes. *Air-Water Gas Transfer, Sel. Papers, Third Int. Symp., Heidelberg University*, ed. by B. Jaehne and E.C. Monahan. Hanau: AEON Verlag & Studio. 1995:37–48.

15. Haltrin V.I., Kattawar G.W. Self-consistent solutions to the equation of transfer with elastic and inelastic scattering in oceanic optics: I. Model. *Applied Optics*. 1993;32(27):5356–5367. https://doi.org/10.1364/AO.32.005356

16. Sukhinov A.I., Protsenko E.A., Chistyakov A.E., Shreter S.A. Comparison of computational efficiencies of explicit and implicit schemes for the problem of sediment transport in coastal water systems. Parallel computing technologies (PaVT'2015). *Proceedings of the international scientific conference*. 2015; 297–307.

17. Sukhinov A.I., Chistyakov A.E., Protsenko E.A. Construction of a discrete two-dimensional mathematical model of sediment transport. *Bulletin of SFedU. Engineering sciences.* 2011;8(121):32–44.

18. Sukhinov A.I., Chistyakov A.E., Bondarenko Yu.S. Estimation of the error in solving the diffusion equation based on schemes with weights. *Bulletin of SFedU. Engineering sciences*. 2011;8(121):6–13.

19. Sukhinov A.I., Belova Y.V., Nikitina A.V., Atayan A.M. Modeling biogeochemical processes in the Azov Sea using statistically processed data on river flow. *Advanced Engineering Research (Rostov-on-Don)*. 2020;20(4):437–445. https://doi.org/10.23947/2687-1653-2020-20-4-437-445

20. Sukhinov A.I., Panasenko N.D. Comparative investigation of neural and locally binary algorithms for image identification of plankton populations. *Computational Mathematics and Information Technologies*. 2022;1(2):70–80. https://doi.org/10.23947/2587-8999-2022-1-2-70-80

21. The official website of Earth observing system. URL: http://eos.com/landviewer/account/pricing (accessed: 01.02.2024).

About the Authors:

Yulia V. Belova, Candidate of Physical and Mathematical Sciences, Associate Professor of the Department of "Mathematics and Computer Science", Don State Technical University (1, Gagarin Sq., Rostov-on-Don, 344003, Russian Federation), ORCID, yvbelova@yandex.ru

Alena A. Filina, Candidate of Technical Sciences, Researcher of Super-Computers and Neurocomputers Research Center (106, Italiansky lane, Taganrog, 347900, Russian Federation), ORCID, j.a.s.s.y@mail.ru

Alexander E. Chistyakov, Doctor of Physical and Mathematical Sciences, Professor of the Department of "Computer Engineering and Automated Systems Software", Don State Technical University (1, Gagarin Sq., Rostov-on-Don, 344003, Russian Federation), ORCID, cheese_05@mail.ru

Claimed Contributorship:
Yu.V. Belova: software implementation, visualization and analysis of calculations.
A.A. Filina: numerical and software implementation, analysis of results.
A.E. Chistyakov: problem statement, development of research methods.

Conflict of Interest Statement: **the authors declare no conflict of interest.**

All authors have read and approved the final manuscript.

Об авторах:
Юлия Валериевна Белова, кандидат физико-математических наук, доцент кафедры математики и информатики Донского государственного технического университета (344003, Российская Федерация, г. Ростов-на-Дону, пл. Гагарина, 1), ORCID, yvbelova@yandex.ru

Алёна Александровна Филина, кандидат технических наук, научный сотрудник ООО «НИЦ супер-ЭВМ и нейрокомпьютеров» (347900, Российская Федерация, г. Таганрог, пер. Итальянский, 106), ORCID, j.a.s.s.y@mail.ru

Александр Евгеньевич Чистяков, доктор физико-математических наук, профессор кафедры программного обеспечения вычислительной техники и автоматизированных систем Донского государственного технического университета (344003, Российская Федерация, г. Ростов-на-Дону, пл. Гагарина, 1), ORCID, cheese_05@mail.ru

Заявленный вклад авторов:
Ю.В. Белова: программная реализация, визуализация и анализ расчетов.
А.А. Филина: численная и программная реализация, анализ результатов.
А.А. Чистяков: постановка задачи, разработка методов исследования.

Конфликт интересов: **авторы заявляют об отсутствии конфликта интересов.**

Все авторы прочитали и одобрили окончательный вариант рукописи.

Received / Поступила в редакцию 11.11.2024
Reviewed / Поступила после рецензирования 26.11.2024
Accepted / Принята к публикации 02.12.2024

INFORMATION TECHNOLOGIES
ИНФОРМАЦИОННЫЕ ТЕХНОЛОГИИ

Check for updates

UDC 004.032.26

Original Theoretical Research

https://doi.org/10.23947/2587-8999-2024-8-4-35-42

Application of Neural Networks for Solving Nonlinear Boundary Problems for Complex-Shaped Domains

Alexander V. Galaburdin
Don State Technical University, Rostov-on-Don, Russian Federation
✉ Galaburdin@mail.ru

Abstract

Introduction. Many practically significant tasks reduce to nonlinear differential equations. In this study, one of the applications of neural networks for solving specific nonlinear boundary problems for complex-shaped domains is considered. Specifically, the focus is on solving a stationary heat conduction differential equation with a thermal conductivity coefficient dependent on temperature.

Materials and Methods. The original nonlinear boundary problem is linearized through Kirchhoff transformation. A neural network is constructed to solve the resulting linear boundary problem. In this context, derivatives of singular solutions to the Laplace equation are used as activation functions, and these singular points are distributed along closed curves encompassing the boundary of the domain. The weights of the network were tuned by minimizing the mean squared error of training.

Results. Results for the heat conduction problem are obtained for various complex-shaped domains and different forms of dependence of the thermal conductivity coefficient on temperature. The results are presented in tables that contain the exact solution and the solution obtained using the neural network.

Discussion and Conclusion. Based on the computational results, it can be concluded that the proposed method is sufficiently effective for solving the specified type of boundary problems. The use of derivatives of singular solutions to the Laplace equation as activation functions appears to be a promising approach.

Keywords: nonlinear boundary problems for complex-shaped domains, neural networks

Acknowledgments. The author expresses gratitude to the editorial staff for their remarks on the formatting, which allowed the article to be made more accessible.

For Citation. Galaburdin A.V. Application of Neural Networks for Solving Nonlinear Boundary Problems for Complex-Shaped Domains. *Computational Mathematics and Information Technologies*. 2024;8(4):35–42. https://doi.org/10.23947/2587-8999-2024-8-4-35-42

Оригинальное теоретическое исследование

Применение нейронных сетей для решения нелинейных краевых задач для областей сложной формы

А.В. Галабурдин
Донской государственный технический университет, г. Ростов-на-Дону, Российская Федерация
✉ Galaburdin@mail.ru

Аннотация

Введение. Многие практически важные задачи сводятся к нелинейным дифференциальным уравнениям. В настоящей работе рассмотрен один из вариантов применения нейронных сетей к решению некоторых нелинейных краевых задач для областей сложной формы, а именно к решению стационарного дифференциального уравнения теплопроводности с коэффициентом теплопроводности, зависящим от температуры.

Материалы и методы. Исходная нелинейная краевая задача сводится к линейной с помощью преобразования Кирхгофа. Нейронная сеть строится для решения полученной линейной краевой задачи. При этом в качестве активационных функций принимаются производные от сингулярных решений уравнения Лапласа, а сингулярные точки этих решений распределены по замкнутым кривым, охватывающим границу области. Для настройки весов сети минимизировалась среднеквадратическая ошибка обучения.
Результаты исследования. Получены результаты решения задачи теплопроводности для различных областей сложной формы и различных форм зависимости коэффициента теплопроводности от температуры. Полученные результаты представлены в виде таблиц, которые содержат точное решение и решение, полученное при помощи нейронной сети.
Обсуждение и заключение. По результатам проведенных расчетов можно сделать вывод о том, что предложенный метод является достаточно эффективным для решения указанного типа краевых задач. Использование в качестве активационных функций производных от сингулярных решений уравнения представляется весьма перспективным.

Ключевые слова: нелинейные краевые задачи для областей сложной формы, нейронные сети

Благодарности. Автор выражает благодарность сотрудникам редакции за указанные замечания по оформлению, которые позволили сделать статью более удобной для восприятия.

Для цитирования. Галабурдин А.В. Применение нейронных сетей для решения нелинейных краевых задач для областей сложной формы. *Computational Mathematics and Information Technologies*. 2024;8(4):35–42. https://doi.org/10.23947/2587-8999-2024-8-4-35-42

Introduction. In constructing models of various natural phenomena, the apparatus of differential equations is often employed. The complexity of the modeled phenomena leads to complex systems of differential equations with intricate domain shapes. Currently, in solving such boundary problems, the method of neural networks is increasingly utilized.

It should be noted that the theoretical foundations of the neural network method were laid in the mid-20th century by A.N. Kolmogorov [1]. The development of the theory in [2] is applied to solving the problem of membrane deflection. In [3], a neural network structure is proposed that allows solving Laplace, Poisson, and heat conduction equations. The numerical solution of the Poisson equation in a two-dimensional domain, obtained by the Galerkin method and Ritz method with deep neural networks, is presented in [4]. In article [5], approaches to solving heat and mass transfer problems based on a perceptron-type neural network are explored.

Recently, there has been a frequent use of physically-informed neural networks to solve partial differential equations [6]. Article [7] presents solutions to classical mechanics problems through the application of physically-informed neural networks. In [8], an approach to solving direct and inverse scattering problems using radial basis function neural networks is discussed. In article [9], based on the method of trust regions, a training method for RBF networks with a customizable functional basis is developed for solving boundary problems in mathematical physics. Article [10] studies the use of physically-informed neural networks in solving unsteady nonlinear differential equations describing the motion of a one-dimensional heat-conducting gas. In works [11, 12], neural networks are applied to solve the Navier-Stokes equations. In works [13, 14], radial basis functions are used as activation functions in the neural network, and their parameters are varied during training.

This work is a development of the approach to solving partial differential equations using neural networks as presented in article [15]. The aim of this study is to develop a method for applying neural networks to solve nonlinear boundary problems for complex-shaped domains.

Materials and Methods. Consider the boundary problem for the nonlinear differential equation

$$\frac{\partial}{\partial x}\left(k(W)\frac{\partial W}{\partial x}\right)+\frac{\partial}{\partial y}\left(k(W)\frac{\partial W}{\partial y}\right)=0 \tag{1}$$

on the planar domain G bounded by a closed curve γ.

This equation describes a stationary thermal field. In this context, W represents the temperature and $k(W)$ represents the thermal conductivity coefficient. Using the Kirchhoff transformation [16, 17], this problem is reduced to a linear form. The essence of the transformation is to introduce a function $u(W)$, such that

$$grad\left(u(W)\right)=\frac{du(W)}{dW}grad(W).$$

Then we have

$$\frac{du(W)}{dW}=k(W) \tag{2}$$

where the original differential equation takes the form of $\Delta u(x, y) = 0$.

From equation (2) we obtain

$$u(x,y)=\int_{w_o}^{W}k(W)\,dW,$$

where W_o is an arbitrary initial quantity.

If the boundary conditions are given for the values of $W = W_o$, on the boundary of the domain, then for u we obtain boundary conditions:

$$u_o=\int_{w_o}^{W_o}k(W)\,dW.$$

Expressing W, gives the solution to the original boundary problem.

Thus, the original nonlinear problem is reduced to a Dirichlet problem, which is solved using a neural network [15]. The basis of the neural network is the relationship:

$$u_i=\frac{1}{2\pi}\sum_{k=1}^{N}c_k\left[\frac{\partial u}{\partial n}\right]_k[U]_{ik}-\frac{1}{2\pi}\sum_{k=1}^{N}c_k[u]_k\left[\frac{\partial U}{\partial n}\right]_{ik}.$$

In this expression $[U]_{ik}$ and $\left[\frac{\partial U}{\partial n}\right]_{ik}$ can be viewed as activation functions, and $c_k\left[\frac{\partial u}{\partial n}\right]_k$ and $c_k[u]_k$ as weights.

Using the least squares method and requiring the specified relationship to hold at each point of the boundary for all functions of the training set, a system of equations can be obtained for determining the weights. To improve the conditioning of this system of equations, it is necessary to increase the singularity of the quantities $[U]_{ik}$ and $\left[\frac{\partial U}{\partial n}\right]_{ik}$, shifting the contour integration a certain distance from the boundary of the domain γ.

The solution to the Dirichlet problem is sought in the form:

$$u(x)=\sum_{k=1}^{N}w_k p(s_k)U(x,\sigma_k)+\sum_{k=1}^{N}v_k p(s_k)V(x,\sigma_k),$$

where $p(s_k)$ — is the value of the unknown function u at the boundary of the domain; $U(x, \sigma_k)$ and $V(x, \sigma_k)$ are activation functions; σ_k and τ_k are points on the closed curves γ_1 and γ_2, that cover the boundary of the domain; γ, x are points in the domain G.

The closed curves γ_1 and γ_2 are similar to the contour γ and are obtained by displacing each point in the direction of the outward normal to the boundary by distances ρ_1 and ρ_2 respectively. During the training process, the weights and values ρ_1 and ρ_2 are determined. To do this, the error functional is minimized:

$$\Pi(w_k,v_k,\rho_1,\rho_2)=\sum_{j=1}^{M}\sum_{i=1}^{N}\left\{\sum_{k=1}^{N}w_k p_k^j U(x_i,\sigma_k)+v_k p_k^j V(x,\sigma_k)-p_k^j\right\}^2$$

where x_i is the coordinate of the i-th point on the boundary contour γ; p_k^j is the boundary value of the j-th function of the training set at the point x_k.

From these relationships, for $\frac{\partial\Pi}{\partial w_m}=0$ and $\frac{\partial\Pi}{\partial v_m}=0$, m = 1,2,...N a system of linear equations is obtained to determine w_m and v_m. The value ρ_1 is determined by simple enumeration, and $\rho_2 = \rho_1+1$.

To assess the accuracy of the obtained solution, the values of u on the boundary of the domain, calculated using the neural network

$$\tilde{u}(s_i)=\sum_{k=1}^{N}w_k p(s_k)U(s_i,\sigma_k)+\sum_{k=1}^{N}v_k p(s_k)V(s_i,\sigma_k)$$

are compared with the specified boundary conditions $u(s)$.

The obtained network parameters do not provide the desired accuracy of the obtained solution. The accuracy can be increased by iterative refinement of the obtained result according to the following scheme:

$$\Delta u^0(s_i)=p(s_i),\ q^0(s_i)=p(s_i),$$

$$\Delta v^{n+1}(s_i)=\sum_{=}^{N}w_k\Delta u^n(s_k)U(s_i,\sigma_k)+\sum_{=}^{N}v_k\Delta u^n(s_k)V(s_i,\tau_k)$$

$$\Delta u^{n+1}(s_i) = \Delta u^{n+1}(s_i) - \Delta v^{n+1}(s_i),\ u_t^{n+1}(s_i) = \Delta u_t^{n+1}(s_i) - \Delta u^{n+1}(s_i),$$

where $u_t^{n+1}(s_i)$ represents the values of the refined solution at the boundary of the domain.

The process of refining the solution continues until the value

$$\frac{\left\|\Delta u^{n+1}(s_i)\right\|}{\left\|u_t^{n+1}(s_i)\right\|}$$

will not be small enough (less than the set value δ_o) or until it starts to grow. The results below are obtained at $\delta_o = 0.0025$.

To determine the value of u at any point x in the domain G use the formula:

$$\tilde{u}(x) = \sum_{k=1}^{N} w_k u_t(s_k) U(x, \sigma_k) + \sum_{k=1}^{N} v_k u_t(s_k) V(s_i, \tau_k).$$

For the training set, a set of functions that are solutions to the Laplace equation was used

$$r^k \cos\left(k \arccos\left(\frac{x}{r}\right)\right) + r^k \sin\left(k \arccos\left(\frac{x}{r}\right)\right),\ r = \sqrt{x^2 + y^2}$$

where $k = 0, 1, 2, 3, \ldots, M$. Calculations were conducted for $M = 75$.

The specified functions were defined in various coordinate systems rotated relative to each other by angles that are multiples of $2\pi/5$.

Activation functions:

$$U(x, y, t, s) = \frac{\beta^5 - 10\beta^3\delta^2 + 5\beta\delta^4 + \delta^5 - 10\delta^3\beta^2 + 5\delta\beta^4}{R^{10}},$$

$$V(x, y, t, s) = \frac{\beta^7 - 21\beta^5\delta^2 + 35\beta^3\delta^4 - 7\beta\delta^6}{R^{10}} n_x + \frac{\delta^7 - 21\delta^5\beta^2 + 35\delta^3\beta^4 - 7\delta\beta^6}{R^{10}} n_y$$

where $\delta = x - t$; $\beta = y - s$; $R = \sqrt{\delta^2 + \beta^2}$; n_x; n_y are the coordinates of the outward normal vector to the boundary of the domain.

Research Results. The proposed method was applied to solve equation (1) for domains whose boundary γ was defined as

$$\begin{cases} x = a\cos(t) + g\sin(\omega t) \\ y = a_1\cos(t) + g_1\sin(\omega t) \end{cases} \quad t \in [0, 2\pi],$$

where a, a_1, g, g_1, ω are variable parameters.

Task 1. Consider the domain $G1$, corresponding to the parameter values: $a = 1.15$; $a_1 = 1.15$; $g = 0.05$; $g_1 = -0.05$; $\omega = 7$ (Fig. 1).

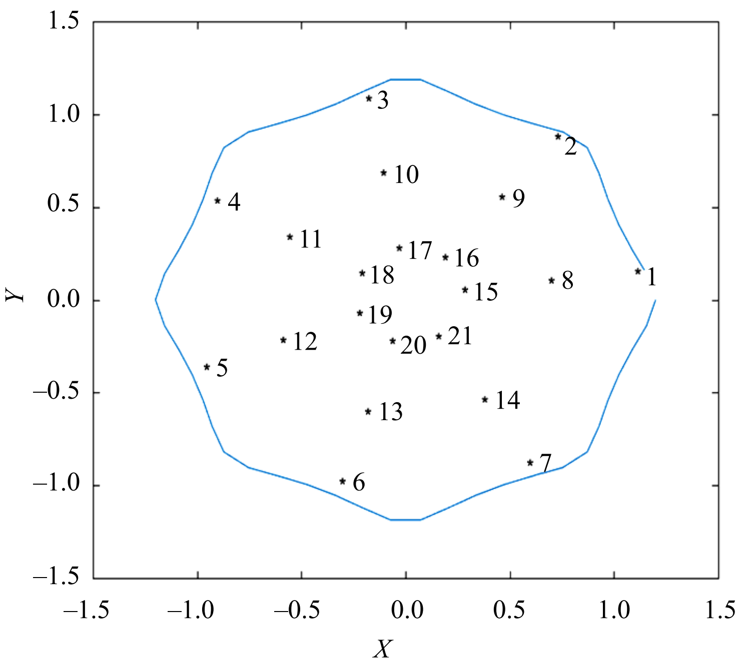

Fig. 1. Domain $G1$

Stars indicate the locations of points in domain $G1$, where the exact solution values and those obtained using the neural network for $\rho_1 = 7$, $\rho_2 = 8$ were calculated.

The equation (1) was considered for the case $k(W) = th(5W)$, which has the exact solution:

$$W_o = arch(11.25((x-1.5)^2 + (y-1.5)^2)^5.$$

The computational results are presented in Table 1.

Task 2. Let us consider domain $G2$ (Fig. 2), corresponding to parameter values $a = 1$; $a_1 = 1$; $g = 0$; $g_1 = 0.3$; $\omega = 3$; $\rho_1 = 10.51$; $\rho_2 = 11.51$.

In equation (1), $k(W) = ch(5W)$, was used, with the exact solution:

$$W_o = arsh(5e^{5x} \sin 5y) / 5.$$

The computational results for this case are presented in Table 2.

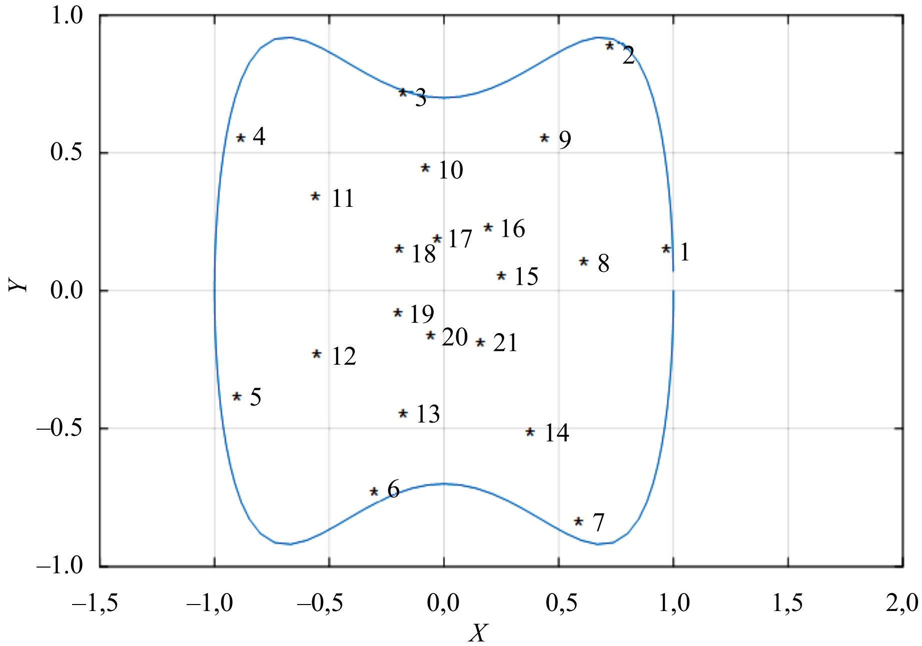

Fig. 2. Domain $G2$

Table 1

Calculation Results

Point No.	1	2	3	4	5	6	7
x	1.0534	0.6865	–0.1869	0.8848	–0.9709	–0.3193	0.5811
y	0.1275	0.8240	1.0218	0.3939	–0.3832	–0.9998	–0.9001
Exact Solution	3.0529	2.6521	2.3621	2.8550	3.3731	3.8462	4.1520
Neural Network Solution	3.0535	2.6479	2.3629	2.8491	3.3771	3.8434	4.1566
Point No.	8	9	10	11	12	13	14
x	0.6937	0.4521	0.1231	–0.5826	–0.6035	–0.1984	0.3612
y	0.0839	0.5426	0.6729	0.3252	–0.2382	–0.6215	–0.5595
Exact Solution	3.2590	3.0804	2.9504	3.1696	3.4495	3.7625	3.9935
Neural Network Solution	3.2584	3.0790	2.9487	3.1681	3.4494	3.7628	3.9947
Point No.	15	16	17	18	19	20	21
x	0.3340	0.2176	–0.0592	–0.2805	–0.2361	–0.0776	0.1413
y	0.0404	0.2612	0.3240	0.1566	–0.0932	–0.2431	–0.2189
Exact Solution	3.5104	3.4526	3.4064	3.4820	3.5887	3.7314	3.8544
Neural Network Solution	3.5100	3.4520	3.4058	3.4815	3.5885	3.7315	3.8547

Table 2

Calculation Results

Point No.	1	2	3	4	5	6	7
x	0.9085	0.6728	–0.1902	–0.8641	–0.9230	–0.3228	0.5679
y	0.1291	0.8320	0.6703	0.5138	–0.4025	–0.7484	0.8587
Exact Solution	0.3489	0.6987	0.6948	0.5361	0.3820	0.2615	0.1561
Neural Network Solution	0.3510	0.6982	0.6941	0.5346	0.3850	0.2666	0.1589
Point No.	8	9	10	11	12	13	14
x	0.5983	0.4430	–0.1253	–0.5690	–0.5737	–0.2006	0.3530
y	0.0850	0.5479	0.4414	0.3383	–0.2502	–0.4652	–0.5338
Exact Solution	0.1849	0.5233	0.5761	0.4537	0.3508	0.29214	0.1806
Neural Network Solution	0.1879	0.5231	0.5753	0.4533	0.3521	0.29578	0.1836
Point No.	15	16	17	18	19	20	21
x	0.2880	0.2133	–0.0603	0.2739	–0.2245	–0.0785	0.1381
y	0.0409	0.2638	0.2125	0.1629	–0.0979	–0.1820	–0.2088
Exact Solution	0.0585	0.2897	0.3780	0.3021	0.2534	0.2496	0.1573
Neural Network Solution	0.0607	0.2901	0.3780	0.3026	0.2544	0.2512	0.1591

Task 3. Consider equation (1) in domain *G*3 (Fig. 3).

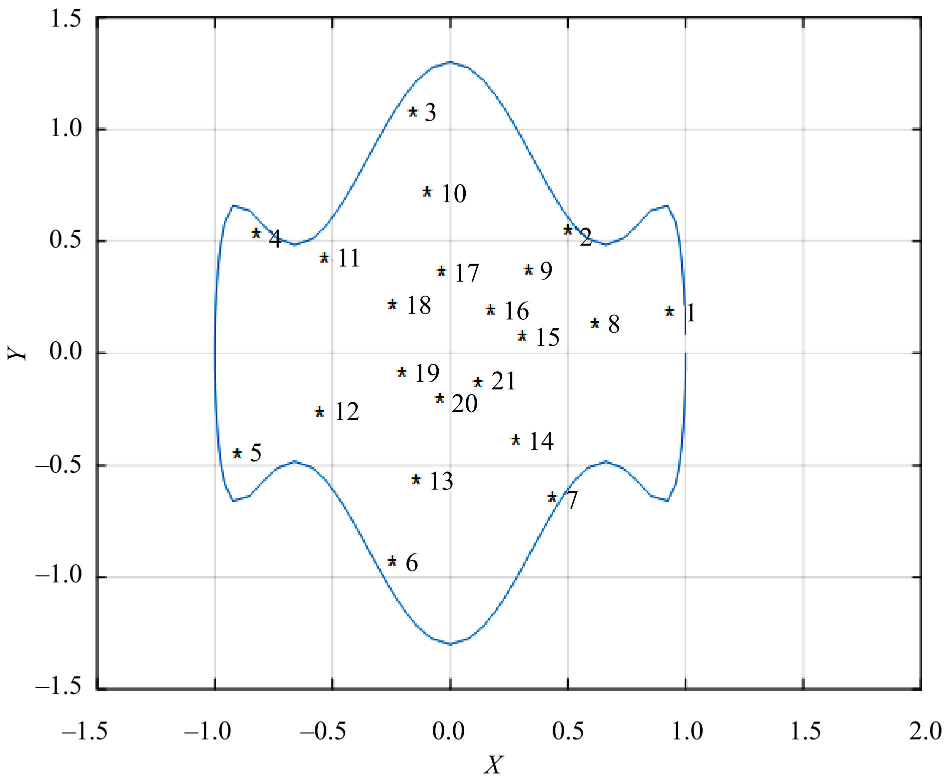

Fig. 3. Domain *G*3

For this case, the parameters are set as follows: $a = 1$; $a_1 = 1$; $g = 0$, $g_1 = 0.3$; $\omega = 5$; $\rho_1 = 11.65$; $\rho_2 = 12.65$. $K(W) = W^{1.5}$, the exact solution is given by:

$$W_o = \left\{2.5\left(\left(x^2 - y^2\right)\cos 1.5x ch1,5y + 2xy \sin 1.5x sh1.5y\right) + 25\sqrt{5}\right\}^{0.4}.$$

The results of the calculations are presented in Table 3.

Table 3

Results of Calculations

Point No.	1	2	3	4	5	6	7
x	0.9090	0.4788	–0.1752	–0.8421	–0.9238	–0.2642	0.4126
y	0.1524	0.5207	1.0491	0.5014	–0.4754	–0.9563	–0.6755
Exact Solution	4.9224	5.0814	4.9816	4.7718	4.7525	4.9738	5.0741
Neural Network Solution	5.0164	5.0845	5.0215	4.8410	4.7800	5.0122	5.1008
Point No.	8	9	10	11	12	13	14
x	0.5986	0.3153	–0.1154	–0.5546	–0.5742	–0.1642	0.2564
y	0.1004	0.3429	0.6908	0.3962	–0.2955	–0.5944	–0.4199
Exact Solution	4.9672	4.9862	4.9595	4.9035	4.8956	4.9575	4.9874
Neural Network Solution	5.0201	5.0286	5.0030	4.9507	4.9375	4.9987	5.0289
Point No.	15	16	17	18	19	20	21
x	0.2882	0.1518	–0.0555	–0.2671	–0.2246	–0.2246	0.1003
y	0.0483	0.1651	0.3326	0.1910	–0.1156	–0.2326	–0.1643
Exact Solution	4.9643	4.9616	4.9576	4.9483	4.9471	4.9575	4.9625
Neural Network Solution	5.0060	5.0049	4.9998	4.9910	4.9893	4.9988	5.0040

Fig. 4 and 5 illustrate the comparison between the exact solution of Problem 3 and the solution obtained using the neural network.

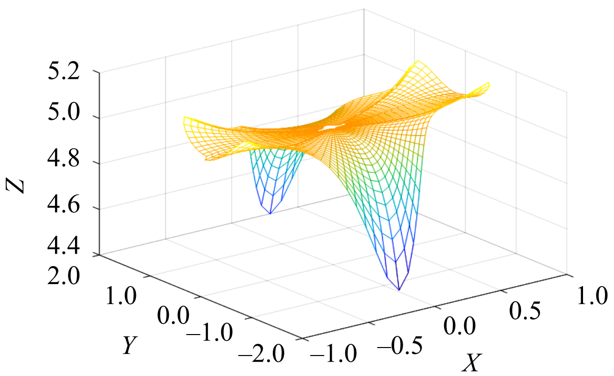

Fig. 4. Exact solution of Problem 3

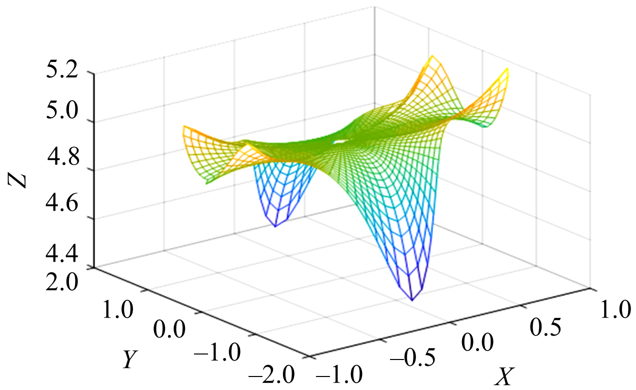

Fig. 5. Solution of Problem 3 obtained using the neural network

Discussion and Conclusion. The presented results advance the approach to solving partial differential equations using neural networks, as outlined in [15]. They convincingly demonstrate the effectiveness of the proposed method for constructing a neural network to solve boundary value problems in domains of complex shape.

This method shows significant potential, making it amenable to further development and refinement for solving a wide range of boundary value problems.

References

1. Kolmogorov A.N. On the representation of continuous functions of several variables in the form of superpositions of continuous functions of one variable and addition. *Reports of the USSR Academy of Sciences*. 1957;114(5):953–956. (In Russ.)

2. Varshavchik E.A., Galyautdinova A.R., Sedova Yu.S., Tarkhov D.A. Solution of partial differential equations for domains with constant boundaries. *Artificial intelligence in solving current social and economic problems of the 21st century: collection of articles. Art. based on materials from the Third All-Russian. scientific-practical conf.* Perm, May 14–18, 2018. Perm. state national research univ.; 2018. P. 294. (In Russ.)

3. Epifanov A.A. Application of deep learning methods for solving partial differential equations. *Advances in cybernetics*. 2020;1(4):22–28. (In Russ.) https://doi.org/10.51790/2712-9942-2020-1-4-3

4. Cai S., Wang Z., Wang S., Perdikaris P., Karniadakis G.E. Physics-informed neural networks for heat transfer problems. *Journal of Heat Transfer*. 2021;143(6): 060801. https://doi.org/10.1115/1.4050542

5. Korsunov N.I., Lomakin A.V. Modeling processes described by a wave differential equation using cellular neural networks. *Scientific bulletins. Series History. Political science. Economy. Informatics*. 2014;15(186):103–107. (in Russ.)

6. Raissia M., Perdikaris P., Karniadakis G.E. Physics-informed neural networks: A deep learning framework for solving forward and inverse problems involving nonlinear partial differential equations. *Journal of Computational Physics*. 2019;378:686–707.

7. Zrelova D.P., Ulyanov S.V. Models of physically informed / aware classical Lagrangian / Hamiltonian neural networks in deep learning. *Modern information technologies and IT education*. 2022;18(2):310–325. (In Russ.) https://doi.org/10.25559/SITITO.18.202202.310-325

8. Shevkun S.A., Samoilov N.S. Application of a neural network approach to solving direct and inverse scattering problems. *Engineering School Bulletin FEFU*. 2021;2(47):210–225. (In Russ.)

9. Gorbachenko V.I., Zhukov M.V. Solving boundary value problems of mathematical physics using radial basis networks. *Journal of Computational Mathematics and Mathematical Physics*. 2017;57(1):133–143. (In Russ.)

10. Kuznetsov K.S., Amosova E.V. Numerical solution of the system of Navier-Stokes equations in the case of a compressible medium using neural networks. *Bulletin of Tomsk State University. Management, computer technology and information science*. 2024;67:31–41. (In Russ.). https://doi.org/10.17223/19988605/67/4

11. Almajid M. Abu-Alsaud M. Prediction of porous media fluid flow using physics informed neural networks. *Journal of Petroleum Science and Engineering*. 2021;208:109205. https://doi.org/10.1016/j.petrol.2021.109205

12. Eivazi H.,Tahani M., Schlatter P., Vinuesa R. Physics-informed neural networks for solving Reynolds-averaged Navier-Stokes equations. *Physics of Fluids*. 2022;34(7):075117. https://doi.org/10.1063/5.0095270

13. Kansa E.J. Motivation for using radial basis functions to solve PDEs. URL: http://uahtitan.uah.edu/kansaweb.html (accessed: 28.11.2024).

14. Kansa E.J. Multiquadrics . A scattered data approximation scheme with applications to computational fluid-dynamics. II. Solutions to parabolic, hyperbolic and elliptic partial differential equations. *Comput. Math. Appl.* 1990;19(8):47–161.

15. Galaburdin A.V. Application of neural networks to solve the Dirichlet problem for areas of complex shape. *Computational Mathematics and Information Technologies*. 2024;8(2):68–79. (In Russ.). https://doi.org/10.23947/2587-8999-2024-8-2-68-79

16. Brebbia K., Telles J., Vroubel L. *Boundary element methods*. Moscow: Mir; 1987. 524 p. (In Russ.)

17. Аккuranov Yu.N., Mikhailov V.N. The method of boundary integral equations for solving nonlinear heat transmission problem. *USSR Comput. Maths. Math. Phys*. 1980;20:117–125.

About the Author:

Alexander V. Galaburdin, Cand. Sci. (Phys. – math.), Associate Professor at the Department Mathematics and informatics, Don State Technical University (1, Gagarin Sq., Rostovon-Don, 344003, Russian Federation), ORCID, Galaburdin@mail.ru

Conflict of Interest Statement: **the author declares no conflict of interest.**

The author has read and approved the final version of manuscript.

Об авторе:

Александр Васильевич Галабурдин, кандидат физико-математических наук, доцент кафедры математики и информатики Донского государственного технического университета (344003, Российская Федерация, г. Ростов-на-Дону, пл. Гагарина, 1), ORCID, Galaburdin@mail.ru

Конфликт интересов: **автор заявляет об отсутствии конфликта интересов.**

Автор прочитал и одобрил окончательный вариант рукописи.

Received / Поступила в редакцию 12.11.2024
Reviewed / Поступила после рецензирования 03.12.2024
Accepted / Принята к публикации 07.12.2024

INFORMATION TECHNOLOGIES
ИНФОРМАЦИОННЫЕ ТЕХНОЛОГИИ

Check for updates

UDC 519.6

Original Empirical Research

https://doi.org/10.23947/2587-8999-2024-8-4-43-48

Identification of Marine Oil Spills Using Neural Network Technologies

Valentina V. Sidoryakina[1,2], **Denis A. Solomakha**[1]

[1] Don State Technical University, Rostov-on-Don, Russian Federation

[2] Taganrog Institute named after A.P. Chekhov (branch) of RSUE, Taganrog, Russian Federation

✉ cvv9@mail.ru

Abstract

Introduction. Detecting oil spills is a critical task in monitoring the marine ecosystem, protecting it, and minimizing the consequences of emergency situations. The development of fast and accurate methods for detecting and mapping oil spills at sea is essential for prompt assessment and response to emergencies. High-resolution aerial photography provides researchers with a tool for remote monitoring of water discoloration. Artificial intelligence technologies contribute to improving and automating the interpretation and analysis of such images. This study aims to develop approaches for identifying oil spilled on water surfaces using neural networks and machine learning techniques.

Materials and Methods. Algorithms capable of automatically identifying marine oil spills were developed using computer image analysis and machine learning methods. The U-Net convolutional neural network was employed for image segmentation tasks. The neural network architecture was designed using the PyTorch library implemented in Python. The AdamW optimizer was chosen for training the network. The neural network was trained on a dataset comprising 8,700 images.

Results. The performance of oil spill detection on water surfaces was evaluated using metrics such as IoU, Precision, Recall, Accuracy, and F1 score. Calculations based on these metrics demonstrated identification accuracy of approximately 83–88%, confirming the efficiency of the algorithms used.

Discussion and Conclusion. The U-Net convolutional network was successfully trained and demonstrated high accuracy in detecting marine oil spills on the given dataset. Future work will focus on developing algorithms using more advanced neural network models and image augmentation methods.

Keywords: marine systems, oil spill detection, aerial photography, deep learning, image segmentation, U-Net, AdamW optimizer

Funding. The study was supported by the Russian Science Foundation grant No. 23–21–00509, https://rscf.ru/project/23-21-00509

For Citation. Sidoryakina V.V., Solomakha D.A. Identification of Marine Oil Spills Using Neural Network Technologies. *Computational Mathematics and Information Technologies*. 2024;8(4):43–48. https://doi.org/10.23947/2587-8999-2024-8-4-43-48

Оригинальное эмпирическое исследование

Идентификация морских разливов нефти на основе нейросетевых технологий

В.В. Сидорякина[1,2] ✉, **Д.А. Соломаха**[1]

[1] Донской государственный технический университет, г. Ростов-на-Дону, Российская Федерация

[2] Таганрогский институт имени А.П. Чехова (филиал) Ростовского государственного экономического университета (РИНХ), г. Таганрог, Российская Федерация

✉ cvv9@mail.ru

Аннотация

Введение. Обнаружение разливов нефти является важной задачей в деле мониторинга состояния морской экосистемы, защиты и минимизации последствий аварийных ситуаций. Для оперативной оценки и реагирования на чрезвычайные ситуации необходима разработка быстрых и точных методов обнаружения и картирования разливов нефти в море. Данные аэрофотосъемки с высоким пространственным разрешением предоставляют исследователям возможность удаленного наблюдения за цветностью вод. Улучшению и автоматизации процедур интерпретации и анализа снимков способствуют технологии искусственного интеллекта. Целью настоящей работы является разработка подходов к идентификации разлившейся на водной поверхности нефти с использованием нейросетей и машинного обучения.

Материалы и методы. Методами компьютерного анализа изображений и машинного обучения созданы алгоритмы, способные автоматически идентифицировать морские разливы нефти. Для задачи сегментации изображений применялась сверточная нейронная сеть U-Net. Для разработки архитектуры нейросети была использована библиотека PyTorch, написанная на языке Python. В качестве оптимизатора нейросети был выбран AdamW. Обучение нейронной сети проводилось с помощью датасета, созданного на основе 8700 изображений.

Результаты исследования. Оценка производительности обнаружения разлитой нефти на водной поверхности выполнена на основе метрик IoU, Precision, Recall, Accuracy и F1 score. Проведенные расчеты с использованием указанных метрик демонстрируют точность идентификации около 83–88 %, что позволяет сделать вывод об эффективности используемых алгоритмов.

Обсуждение и заключение. Сверточная сеть U-Net успешно обучена и способна давать высокую точность при обнаружении морских разливов нефти на заданном датасете. Перспективами дальнейших работ авторов является создание алгоритмов с использованием более сложной нейросетевой модели и методов аугментации изображений.

Ключевые слова: морские системы, обнаружение разлива нефти, аэрофотоснимки, глубокое обучение, сегментация изображений, U-Net, оптимизатор AdamW

Финансирование. Исследование выполнено за счет гранта Российского научного фонда № 23–21–00509, https://rscf.ru/project/23-21-00509

Для цитирования. Сидорякина В.В., Соломаха Д.А. Идентификация морских разливов нефти на основе нейросетевых технологий. *Computational Mathematics and Information Technologies*. 2024;8(4):43–48. https://doi.org/10.23947/2587-8999-2024-8-4-43-48

Introduction. Oil spills are one of the primary sources of marine pollution, exerting a negative impact on aquatic ecosystems. Toxic chemicals present in oil can persist in the water column for extended periods and may even settle on the seabed, influencing sedimentation rates. Oil spills may occur intentionally, for example, when cargo ships transporting oil discharge waste oil and bilge water into the sea. However, most oil spills are accidental and generally result from emergencies whose time, location, and scale are difficult to predict. Examples include tanker accidents and leaks from offshore installations. Detecting and promptly addressing the consequences of oil spills require a set of modern monitoring methods for marine ecosystems, characterized by high accuracy and efficiency [1, 2].

The identification of marine oil spills using neural network technologies has gained significant importance in recent years for monitoring the ecological status of water bodies. Neural networks enable the efficient processing of large volumes of data, allowing for real-time detection of changes on the ocean surface [3]. Deep learning algorithms can identify patterns characteristic of oil spills, even in the presence of complex backgrounds and noisy data. The use of such technologies not only enhances the speed of detection but also facilitates more accurate predictions of potential contamination zones.

Significant progress has been made in global research on identifying oil spills on water surfaces using neural network technologies [4–9]. Despite these advancements, challenges remain in the recognition of such structures in marine environments, necessitating further research and development. This study is dedicated to addressing these challenges within this field of research.

Materials and Methods. To address the task of segmenting images of oil spills on the sea surface, the study employs the U-Net convolutional neural network for deep learning. This choice was made based on a comparative analysis of U-Net with other networks such as FCN32, SegNet, and DilatedSegNet for recognizing structures on water surfaces [10, 11]. The network architecture was developed using the PyTorch library, implemented in Python.

Optimization methods play a crucial role in artificial neural networks, significantly influencing the training process. The final accuracy of a neural network depends on aligning the weights of artificial neurons with the loss function, which must be minimized with each epoch. Faster convergence to the global minimum enhances recognition accuracy and reduces training time. AdamW, one of the most effective optimization algorithms for training neural networks, was selected as the optimizer. AdamW adjusts the learning rate for each network weight individually during training. A modified gradient descent algorithm was applied to minimize the loss function. The following parameters were used: batch size — 64, momentum — 0.9, and learning rate — 0.001.

The neural network was trained on a dataset comprising 8,700 images obtained through aerial photography. Before training, the data were split into the following subsets: 90 % for training, 5 % for validation, and 5 % for testing.

Fig.1 and 2 present the accuracy and loss graphs during the training and validation stages of the neural network model.

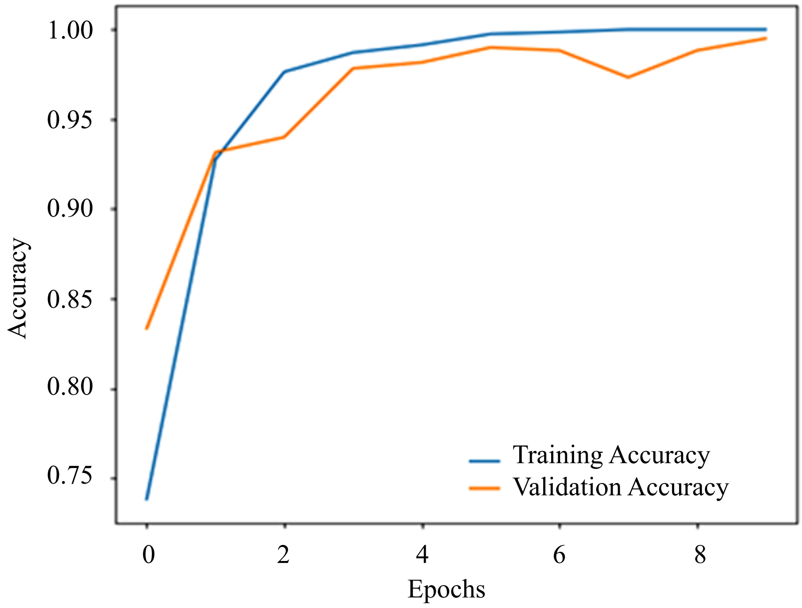

Fig. 1. Accuracy graph during neural network training

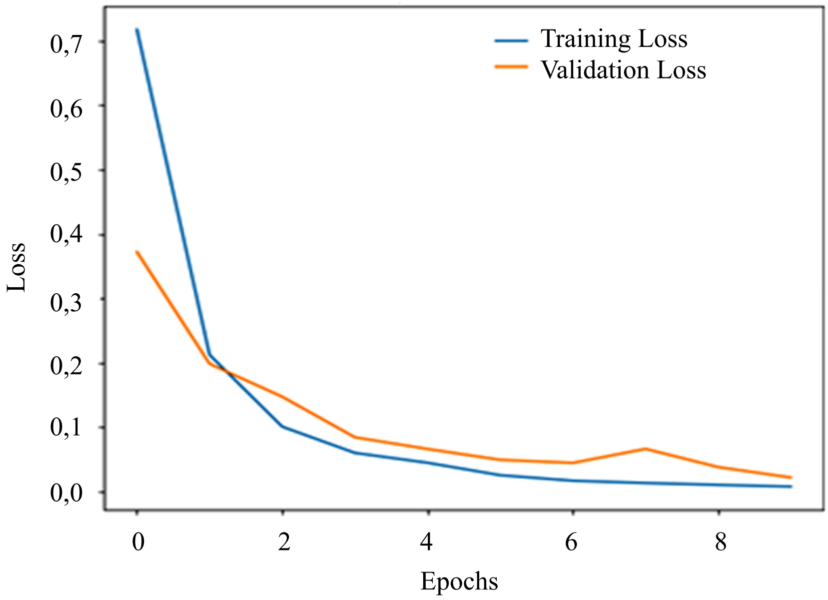

Fig. 2. Loss function graph during neural network training

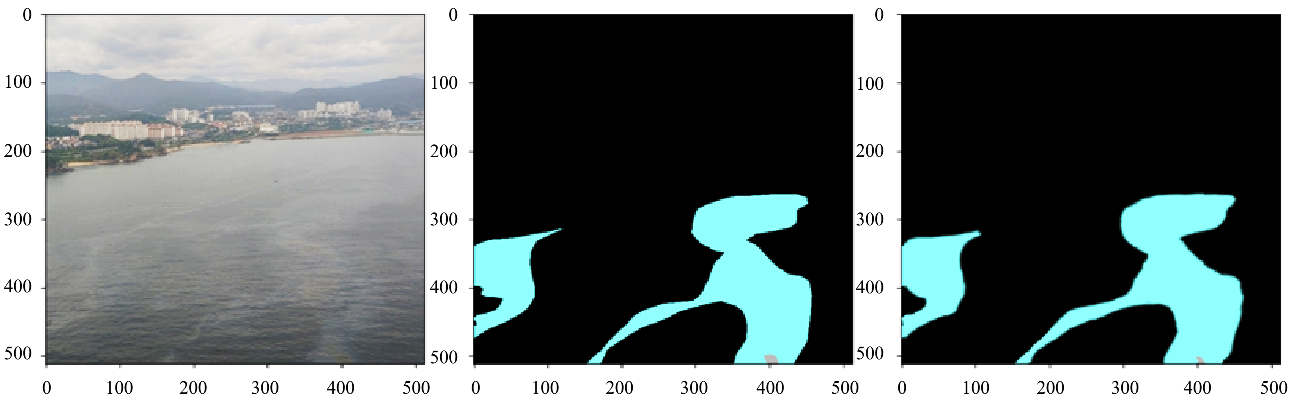

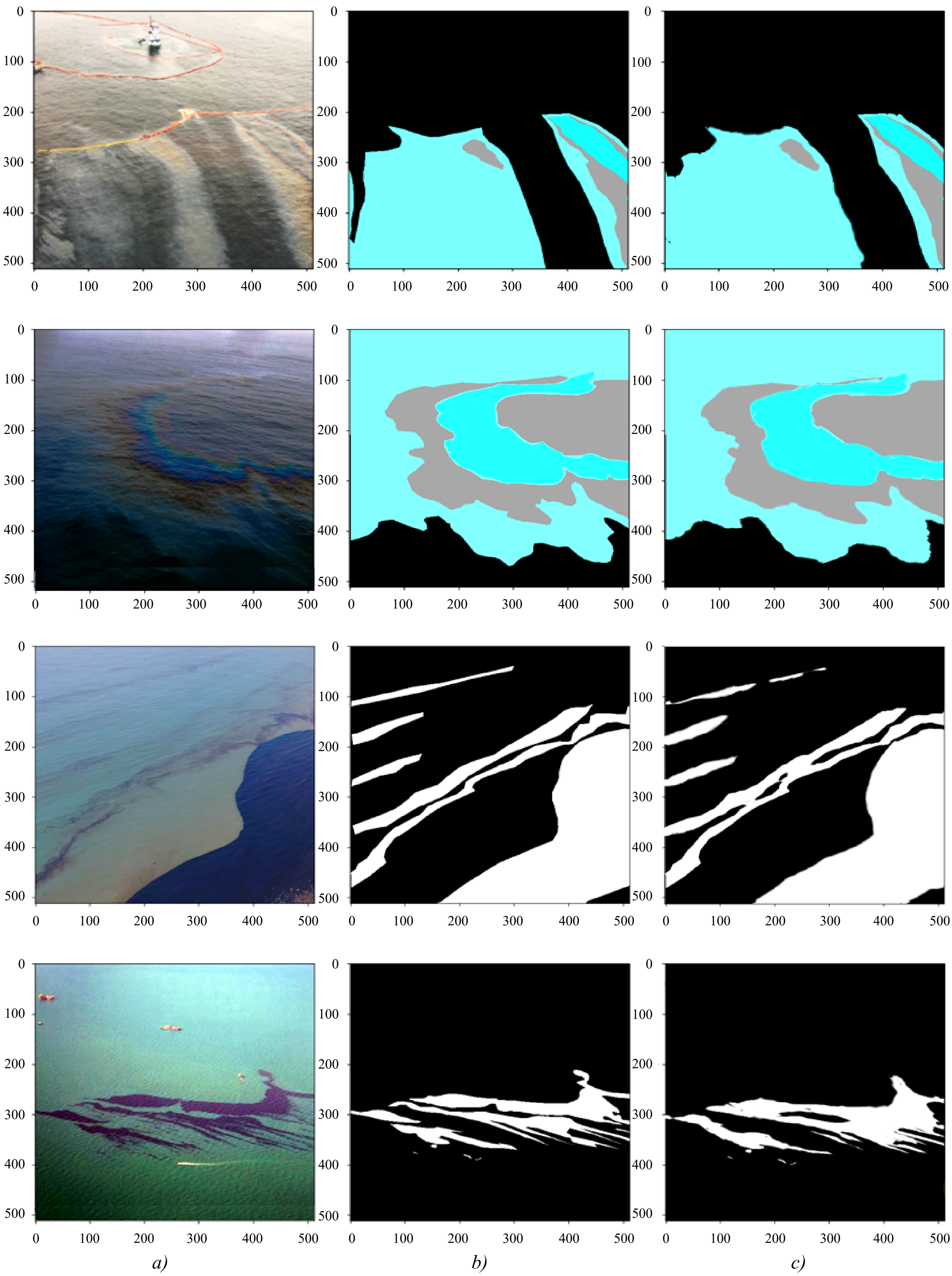

Fig. 3. Numerical experiments conducted on aerial photographs:
a — Input images; *b* — Image masks; *c* — Segmentation results

For color-based segmentation, the RGB model was used, incorporating the following values: Rainbow oil (55, 255, 255), silver oil (155, 255, 255), brown oil (180, 180, 180), black oil (0, 0, 0), and background (255, 255, 255). A specific spectrum was selected to identify each oil type.

To evaluate the performance of the automated classifiers, widely used metrics in detection and segmentation tasks were applied, including IoU, Precision, Recall, Accuracy, and F1 score.

Table 1

Model Accuracy for the Dataset Under Study

Neural Network Model	IoU	Precision	Recall	Accuracy	F1 score
Detection Accuracy of Oil Spills from Aerial Photographs	0.83	0.86	0.88	0.85	0.87

The data from Table 1 indicates that the achieved accuracy using the mentioned metrics ranges from 83 % to 88 %, demonstrating not only successful detection of oil spills but also their type identification — an aspect that is significantly overlooked in this field of study. Calculations were performed using an NVIDIA GeForce RTX 4090 graphics processor.

Discussion and Conclusion. The results of this study address the challenge of detecting and segmenting marine oil spills using deep learning structures. Semantic segmentation was performed using a fully convolutional U-Net network. The recognition accuracy for these structures on the water surface was over 83 % (as calculated using metrics such as IoU, Precision, Recall, Accuracy, and F1 score), showcasing the effectiveness of the employed algorithms.

Future work by the authors includes the development of algorithms using more complex neural network models and image augmentation methods. The authors extend their gratitude for the extensive dataset provided by international colleagues [12], which enabled the experimental part of this study.

References

1. Sidoryakina V.V. Mathematical model of the process of oil pollution spreading in coastal marine systems. *Computational Mathematics and Information Technologies*. 2023;7(4):39–46. (In Russ.). https://doi.org/10.23947/2587-8999-2023-7-4-39-46

2. Sidoryakina V., Filina A. A set of tools for predictive modeling of the spatial distribution of oil pollution. *E3S Web of Conferences*. 2024;592:04017. https://doi.org/10.1051/e3sconf/202459204017

3. Muratov M.V., Konov D.S., Petrov D.I., Petrov I.B. Application of convolutional neural networks for searching and determining physical characteristics of heterogeneities in the geological environment based on seismic data. *Mathematical notes of NEFU*. 2023;30(1):101–113. (In Russ.). https://doi.org/10.25587/SVFU.2023.87.50.008

4. Huang X., Zhang B., Perrie W., Lu Y., Wang C. A novel deep learning method for marine oil spill detection from satellite synthetic aperture radar imagery. *Marine Pollution Bulletin*. 2022;179:11366. https://doi.org/10.1016/j.marpolbul.2022.113666

5. Rousso R., Katz N., Sharon G., Glizerin Y., Kosman E., Shuster A. Automatic Recognition of Oil Spills Using Neural Networks and Classic Image Processing. *Water*. 2022;14:1127. https://doi.org/10.3390/w14071127

6. Favorskaya M., Nishchhal N. Verification of Marine Oil Spills Using Aerial Images Based on Deep Learning Methods. *Informatics and Automation*. 2022; 21(5):937–962. https://doi.org/10.15622/ia.21.5.4

7. Zeng K., Wang Y. A Deep Convolutional Neural Network for Oil Spill Detection from Spaceborne SAR Images. *Remote Sens.* 2020;12:1015. https://doi.org/10.3390/rs12061015

8. Yekeen S.T., Balogun A.L. Automated Marine Oil Spill Detection Using Deep Learning Instance Segmentation Model. *Int. Arch. Photogramm. Remote Sens. Spatial Inf. Sci*. 2020;XLIII-B3-2020:1271–1276. https://doi.org/10.5194/isprs-archives-XLIII-B3-2020-1271-2020

9. Safin M.A., Bikbulatov R.I., Pirogova A.M. Improving the efficiency of automatic identification of oil spills using unmanned aerial vehicles. *Engineering Bulletin of the Don*. 2022;12. (In Russ.). URL: ivdon.ru/ru/magazine/archive/n12y2022/8046 (accessed: 25.11.2024).

10. Sukhinov A., Sidoryakina V., Solomakha D. Identification of plankton populations in the surface waters of the Azov Sea based on neural network structures of various architectures. *BIO Web of Conferences*. 2024;141:03003. https://doi.org/10.1051/bioconf/202414103003

11. Sukhinov A.I., Sidoryakina V.V., Solomakha D.A. Identification of plankton populations on the surface of marine systems based on machine learning methods. *Priority areas for the development of science and education in the context of the formation of technological sovereignty: materials of the International scientific and practical conference*. Rostov-on-Don: DSTU-Print; 2024. P. 272–277. (In Russ.)

12. Bui N.A., Oh Y.G., Lee I.P. Oil spill detection and classification through deep learning and tailored data augmentation. *International Journal of Applied Earth Observation and Geoinformation*. 2024;129:103845. https://doi.org/10.1016/j.jag.2024.103845

About the Authors:

Valentina V. Sidoryakina, Cand. Sci. (Phys. – math.), Associate Professor at the Department of Mathematics and Computer Science, Don State Technical University (1, Gagarin Sq., Rostov-on-Don, 344003, Russian Federation); Associate Professor at the Department of Mathematics and Physics, Taganrog Institute named after A.P. Chekhov (branch) of RSUE (RINH) (347936, Russian Federation, Taganrog, Initsiativnaya Str., 48), ORCID, SPIN-code, ResearcherID, MathSciNet, ScopusID, cvv9@mail.ru

Denis A. Solomakha, 4th year student at the Department of Mathematics and Computer Science, Don State Technical University (1, Gagarin Sq., Rostov-on-Don, 344003, Russian Federation), SPIN-code, solomakha.05@yandex.ru

Claimed Contributorship: **the authors contributed equally to this article.**

Conflict of Interest Statement: **the authors declare no conflict of interest.**

All authors have read and approved the final manuscript.

Об авторах:

Валентина Владимировна Сидорякина, кандидат физико-математических наук, доцент кафедры математики и информатики Донского государственного технического университета (344003, Российская Федерация, г. Ростов-на-Дону, пл. Гагарина, 1); доцент кафедры математики и физики Таганрогского института имени А.П. Чехова (филиала) Ростовского государственного экономического университета (347936, Российская Федерация, г. Таганрог, ул. Инициативная, 48), ORCID, SPIN-код, ResearcherID, MathSciNet, ScopusID, cvv9@mail.ru

Денис Анатольевич Соломаха, студент кафедры математики и информатики Донского государственного технического университета (344003, Российская Федерация, г. Ростов-на-Дону, пл. Гагарина, 1), SPIN-код, solomakha.05@yandex.ru

Заявленный вклад авторов: **все авторы сделали эквивалентный вклад в подготовку публикации.**

Конфликт интересов: **авторы заявляют об отсутствии конфликта интересов.**

Все авторы прочитали и одобрили окончательный вариант рукописи.

Received / Поступила в редакцию 30.10.2024
Reviewed / Поступила после рецензирования 29.11.2024
Accepted / Принята к публикации 06.12.2024